Journal of Medicinal Chemistry

pubs.acs.org/jmc

Article

Antibiotic Conjugates with an Artificial MECAM-Based Siderophore Are Potent Agents against Gram-Positive and Gram-Negative Bacterial Pathogens

Lukas Pinkert, Yi-Hui Lai, Carsten Peukert, Sven-Kevin Hotop, Bianka Karge, Lara Marie Schulze, Jörg Grunenberg, and Mark Brönstrup*

Cite This: *J. Med. Chem.* 2021, 64, 15440−15460

Read Online

ACCESS | Metrics & More | Article Recommendations | Supporting Information

ABSTRACT: The development of novel drugs against Gram-negative bacteria represents an urgent medical need. To overcome their outer cell membrane, we synthesized conjugates of antibiotics and artificial siderophores based on the MECAM core, which are imported by bacterial iron uptake systems. Structures, spin states, and iron binding properties were predicted *in silico* using density functional theory. The capability of MECAM to function as an effective artificial siderophore in *Escherichia coli* was proven in microbiological growth recovery and bioanalytical assays. Following a linker optimization focused on transport efficiency, five β-lactam and one daptomycin conjugates were prepared. The most potent conjugate **27** showed growth inhibition of Gram-positive and Gram-negative multidrug-resistant pathogens at nanomolar concentrations. The uptake pathway of MECAMs was deciphered by knockout mutants and highlighted the relevance of FepA, CirA, and Fiu. Resistance against **27** was mediated by a mutation in the gene encoding ExbB, which is involved in siderophore transport.

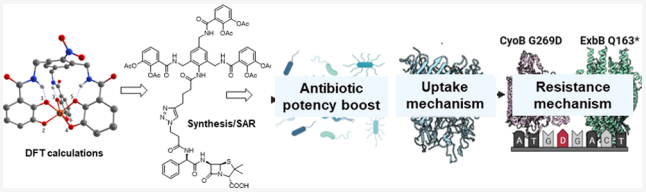

INTRODUCTION

The rising resistance of human pathogenic bacteria to clinically used antibiotics has become a worldwide health problem that is associated with severe medical and economic consequences. It is striking that in a consensus list on the most critical pathogens, established by the WHO,[1] top priority was assigned to Gram-negative bacteria, *i.e.*, drug-resistant congeners of *Acinetobacter baumannii*, *Pseudomonas aeruginosa*, and *Enterobacteriaceae*. The fact that therapeutic options against them are particularly limited[2] is due to their outer cell membrane, which represents a tight, impermeable biological barrier against antibiotic agents.[3−5] A promising strategy to enhance translocation across the outer cell membrane is to embark on bacterial internalization systems, like those for siderophore transport.[6] Siderophores are small-molecule iron chelators synthesized and secreted by prokaryotes. Iron-loaded siderophores are actively transported across the bacterial outer membrane, thus satisfying the bacterial demand for iron.[7,8] In a so-called "Trojan Horse" strategy,[9] antibiotic molecules have been conjugated to siderophores and thereby reach much higher intracellular concentrations compared to the free drugs.[10,11] After decades of research and development, a successful clinical validation of this principle has been reached with the siderophore-containing cephalosporin "*Cefiderocol*" (*Fetroja*), which has recently obtained market authorization.[12,13]

Enterobactin (**1**), the main siderophore of *Escherichia coli*,[14,15] possesses a chiral trilactone core that provides a preorientation of the three iron-chelating catechol groups (Scheme 1), thus minimizing molecular strain when forming an octahedral complex with ferric iron. Hence, it is one of the strongest natural iron binders known and became the prototype model for siderophore uptake and conjugation studies.[16,17] Because the synthetic access to enterobactin conjugates is demanding at a large scale, and because the trilactone backbone is reported to be unstable,[18] we aimed to replace enterobactin's trilactone core by more durable, synthetic moieties. The principal feasibility of this approach has been demonstrated by Miller and others;[16,19−24] we qualified the DOTAM core **2** as a suitable scaffold recently.[25] In many cases, the catechols are masked as acetylated prodrugs to avoid *in vivo* deactivation of the iron-chelating units by catechol-*O*-methyltransferases.[26] In this study, we explored a simple benzene ring to accommodate three arms for iron binding and a fourth arm for antibiotic payload attachment. In early reports, 1,3,5-*N*,*N*′,*N*″-tris-(2,3-dihydroxybenzoyl)-triaminomethylbenzene (MECAM, **3**, Scheme 1)[27,28] has been shown to effectively transport ferric iron through the outer membrane of Gram-negative *E. coli* into the periplasmic space.[29,30]

Received: August 20, 2021
Published: October 8, 2021

Scheme 1. Chemical Structures of Enterobactin (1), and Artificial Siderophores with DOTAM- (2), and MECAM-Based (3) Cores

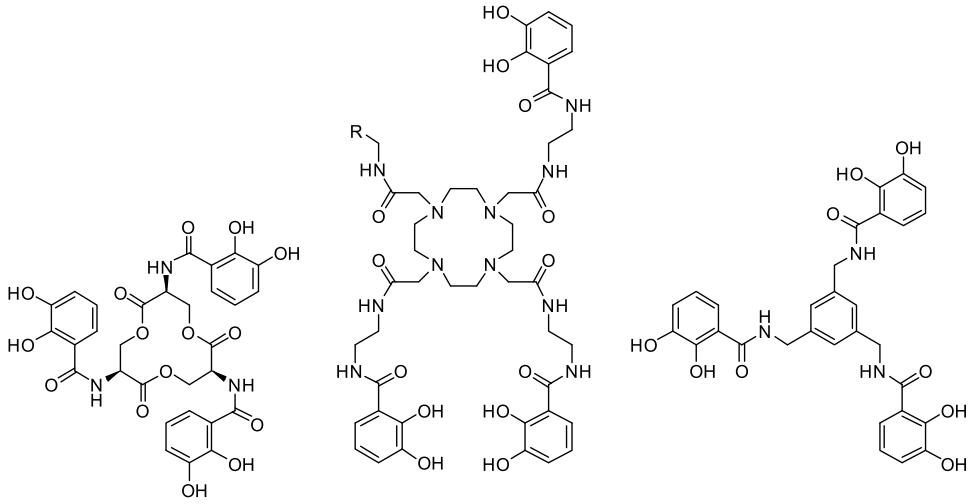

In this study, we systematically varied the linkers branching from the benzene core, synthesized first MECAM-based antibiotic conjugates, and characterized their structural, microbiological, and antibiotic properties, as well as their uptake routes and resistance mechanisms in *E. coli*.

RESULTS

MECAM Scaffold Is Amenable to Structural Variations and Functionalization. MECAM, the starting point for our studies, already possessed three catechol units for iron binding. Because the attachment of a fourth arm was required to install an antibiotic payload *via* a linker,[31] we chose to introduce a nitro group for this purpose, whose subsequent reduction should give rise to an easily accessible amine function. The acyl-protected siderophore **8** was synthesized starting from 1,3,5-tris(bromomethyl)benzene **7** by nitration, a trifold amine substitution, and the attachment of acid chloride **6**. To assess the roles of the nitro group and of the acetyl-protecting groups, compounds **9**−**11** were prepared as well (Scheme 2).

To investigate whether structural modifications of MECAM had an impact on its iron transport capabilities, we designed a set of derivatives with increasing distances between the aromatic core and the iron-chelating units. While elongation of the MECAM catechol arms may decrease conformational strain in the respective ferric iron complexes, the growing number of degrees of freedom renders the formation of such complexes entropically unfavorable at the same time.

To elucidate the structural boundaries for bioactive siderophores, four compounds **12**−**15** were synthesized, thereby covering arm length between three atoms (as in **8**) and seven atoms (as in **15**) linking the central and the peripheral phenyl rings (Schemes S1−S3). Furthermore, three MECAM-derived congeners **16**−**18** could be obtained, in which the 1,3,5-substitution pattern is replaced by a 1,2,3-substitution pattern, thus increasing steric demand and changing symmetry properties (Schemes S4 and S5).

MECAM-Based Siderophores Bind Iron in Different Spin States. The structural and energetic properties of the synthetic siderophores were examined next. Since we were especially interested in the impact of linker length on iron coordination, the substances with the shortest and longest distances between aromatic core and catechol units, **10**, **19**, and **20** (Scheme 2) were studied *in silico* by density functional theory (DFT) applying the hybrid version of the TPSS functional.[32] The TPSS functional provides only 10% exact exchange, reducing the large systematic error in other functionalities when it comes to the description of the electronic configuration in transition-metal complexes. Since an *ab initio* prediction of the thermodynamic stabilities in solution would be far too challenging because of the structural variance in our studied systems, we additionally characterized the stability (or lability) of the Fe−O contacts by computing all relevant relaxed force constants.[33,34] As the hydroxyl groups of catechols were fully deprotonated, the complexes had an overall charge state of −3. After a manual conformational search followed by individual geometry optimizations, we ended up with relaxed structures for the iron−siderophore complexes exemplified here for the siderophore **10** (Figure 1A). All octahedral ferric iron complexes were found to represent minima of the potential energy surface characterized by additional calculations of the second energy derivatives (no imaginary frequencies). In the octahedral ferric iron complex **10**, the distances between ferric iron and oxygen atoms differ between the 2- and 3-positions of the three catechols, the latter ones adopting values close to 2.0 Å (Table S1). Due to the formation of an intramolecular hydrogen bond,[35] electron density is withdrawn from the oxygens in 2-positions (O1, O3, and O5 in Table S1), resulting in a Fe−O bond elongations of *ca.* 0.1 Å. Correspondingly, our calculated relaxed force constants are lower and the kinetic lability should be more pronounced for these FeO distances. Our findings imply that the iron complex with siderophore **10** nearly adapts an ideal C_3 symmetry (Figure 1A).

In a second step, total energies were computed for the Fe(III) high-spin and low-spin adducts of **10**, **19**, and **20** as well for some natural siderophore−iron complexes (Figure S1), respectively. To our knowledge, octahedral low-spin complexes have not been reported for any siderophore so far in the literature. And indeed, our analysis of common natural siderophores and of **10** depicted an energetic preference of the high-spin configuration. To our surprise, the synthetic siderophore **19** was found to favor the low-spin state (ΔE

https://doi.org/10.1021/acs.jmedchem.1c01482
J. Med. Chem. 2021, 64, 15440−15460

Scheme 2. Syntheses of MECAM Siderophores 8−11, and Structures of the Final Products 12−20[a]

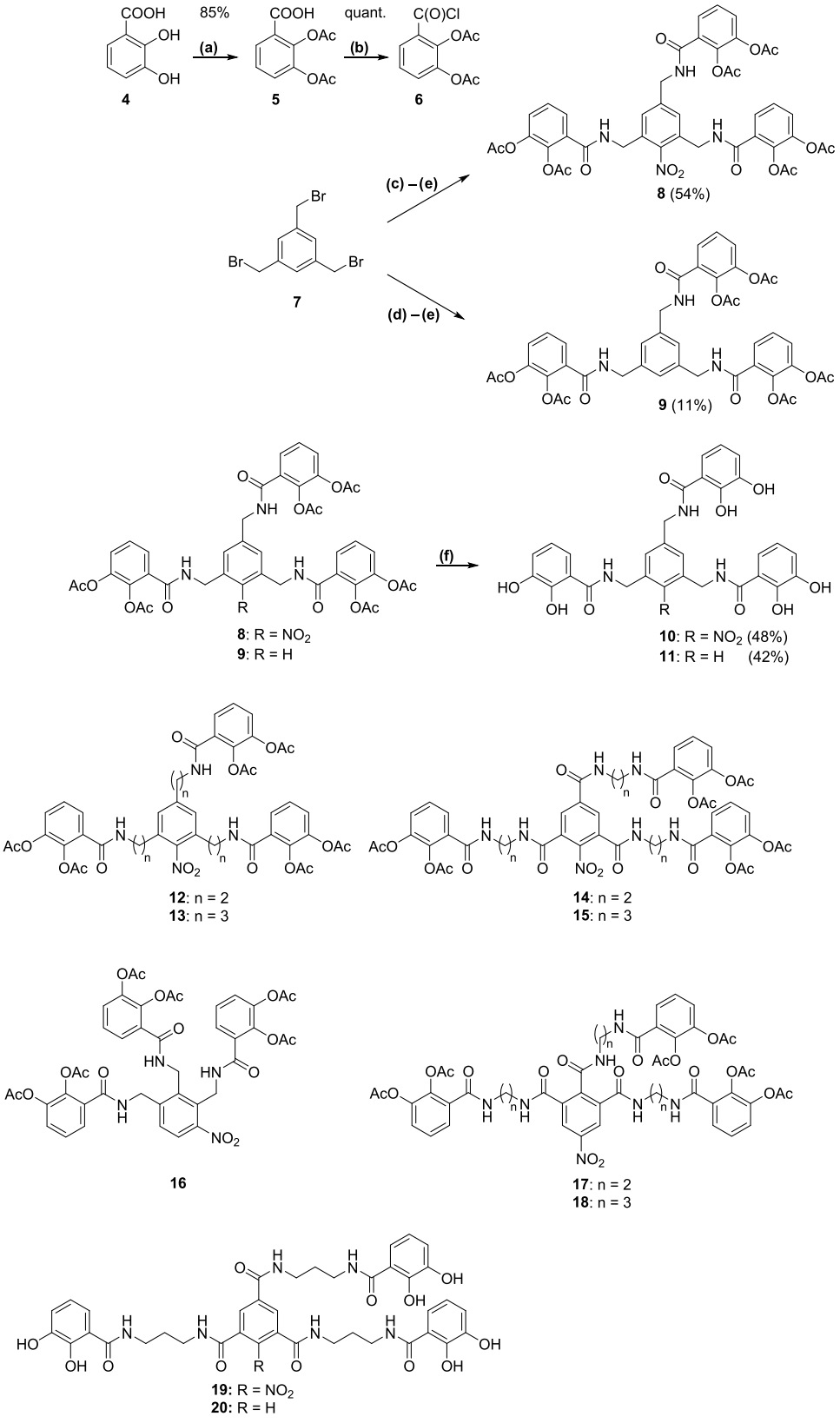

[a]Reagents and conditions: (a) Ac_2O, DMAP, NEt_3, reflux, 3 h; (b) $(COCl)_2$, DMF, CH_2Cl_2, 0 °C → rt, 2.5 h; (c) HNO_3, H_2SO_4, 0 °C → rt, 1 day; (d) $NH_{3(aq)}$, EtOH, THF, rt, 1 day; (e) **6**, $KHCO_3$, H_2O, 1,4-dioxane, 0 °C → rt; (f) $KOH_{(aq)}$, rt, 1 h.

(hs − ls) = 41.9 kJ/mol) as the electronic ground state of the complexed iron(III) ion. This finding is of importance since a low-spin ground state should be associated with a pronounced kinetic stability of the complex (see the analysis below). A

https://doi.org/10.1021/acs.jmedchem.1c01482
J. Med. Chem. 2021, 64, 15440−15460

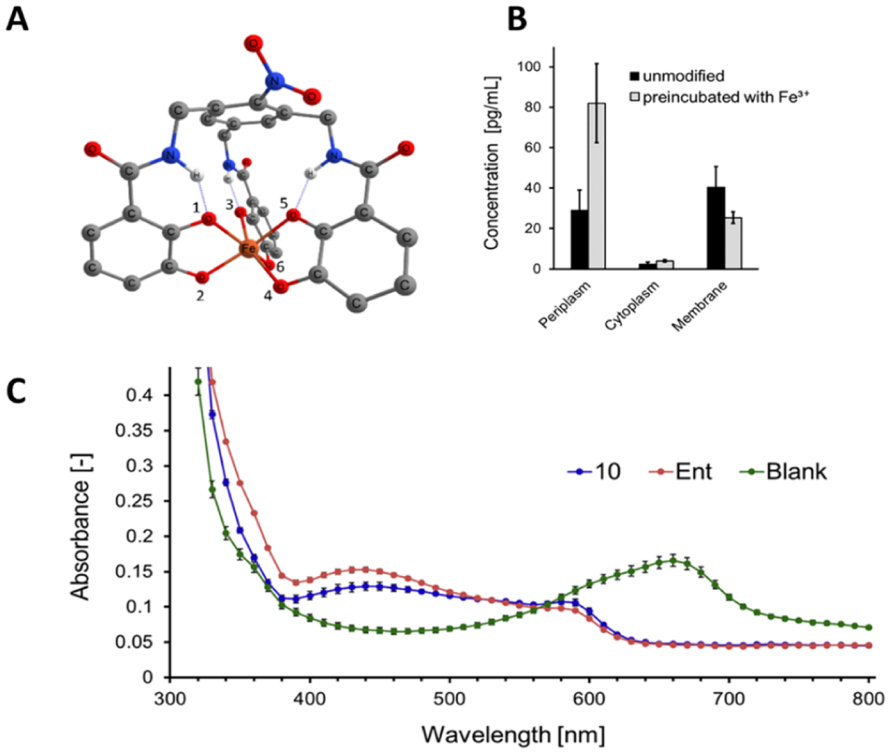

Figure 1. Characterization of **10**. (A) Calculated DFT structure of ferric iron complex in stick representation with colorized atoms of carbon (gray), oxygen (red), and iron as well as nitrogen (blue). (B) Absorption spectra of a Fe^{3+}-CAS solution following addition of **10** or enterobactin (Ent). (C) Intracellular concentration of **10** in *E. coli*. Following the incubation of *E. coli* with **10** (with or w/o Fe^{3+}), bacterial subcompartments were fractionated, and the amount of **10** was quantified by LC-MS/MS. Compound **10** was mainly present in the periplasm and membranes but barely in the cytoplasm.

direct conformational influence of the aromatic nitro group (note the two additional stabilizing NH...O(nitro) interactions, Figure S1) on the electronic ground state of the complex is apparent because the respective desnitro analogue **20** again has a high-spin ground state (ΔE (hs − ls) = −38.5 kJ/mol). We speculate that, in solution, these additional intramolecular hydrogen bonds will be weakened. Nevertheless, siderophore **19** seems to be a good starting point, which might lead to a new class of kinetic stabilized low-spin siderophores.

The iron−oxygen distances of **19** and **20** are smaller and more homogeneous for the low-spin state compared to the respective high-spin complexes (Table S1). The force constants, indicators of the kinetic lability of weakly bound complexes, are significantly higher, suggesting that the low-spin configuration is kinetically more inert. The average force constant of 0.97 N/cm for the preferred high-spin configuration of **20** is comparable to the value of 0.95 N/cm that was recently reported for the natural siderophore enterobactin.[36] The average relaxed force constant of **19** is higher (1.16 N/cm, +0.19 N/cm compared to **20**) in the high-spin state, and this difference is even more pronounced in the preferred low-spin state of **19** (2.01 N/cm, +0.31 compared to **20**). As expected, the unusual preference of the low-spin configuration is reflected by relatively strong and covalent siderophore−iron bonds.

The length of the linker had no impact on the average Fe−O bond length, as reflected by identical values of 2.04 Å for the high-spin complexes of **10** and **20**, and also their average force constants were comparable (1.03 *vs* 0.97 N/cm, respectively). However, the distortion from an ideal C_3-symmetry was larger for the siderophores with longer linkers.

Next, the ability of MECAM siderophores **10** to form stable complexes with ferric iron was probed experimentally in a colorimetric assay utilizing chrome azurol S (CAS). CAS is a red dye, which forms blue complexes with ferric iron. The withdrawal of ferric iron from CAS by strong iron chelators like the positive control enterobactin results in a colorimetric shift from blue to red. We observed that the absorption maximum of CAS-Fe^{3+} at around 660 nm, corresponding to a blue color, vanished after the addition of **10** (Figure 1C). This demonstrates that the nitro compound **10** was capable of chelating a ferric iron.

MECAM-Based Siderophores Transport Iron into the Periplasm *via* FepA. The ability to bind iron is a necessary but not sufficient condition to serve as an artificial siderophore for Gram-negative bacteria. To probe whether the compounds would function as a siderophore, a growth recovery assay with an *E. coli* Δ*entA* strain was conducted. This strain is not able to biosynthesize its endogenous siderophore enterobactin and thus is only able to grow under iron-limited conditions when a suitable (xeno-)siderophore is added (Figure 2A, dimethyl sulfoxide (DMSO) and enterobactin controls). Each of the compounds **8**−**11** restored growth sufficiently, illustrating the aptness of MECAM to serve as an iron carrier for *E. coli* in its free and its acetylated prodrug form (Figure 2A).

The growth recovery assay with the artificial siderophores **8** and **12**−**18** showed that only compounds **8** and **16**, possessing the shortest linkers between the aromatic ring and catechol units, were accepted as xenosiderophores by *E. coli* (Figure 2B). For siderophores **19** and **20**, deacetylated congeners of compound **15**, the ability to form complexes with ferric iron had been observed (*v.i.*). Thus, increasing the distances

https://doi.org/10.1021/acs.jmedchem.1c01482
J. Med. Chem. 2021, 64, 15440−15460

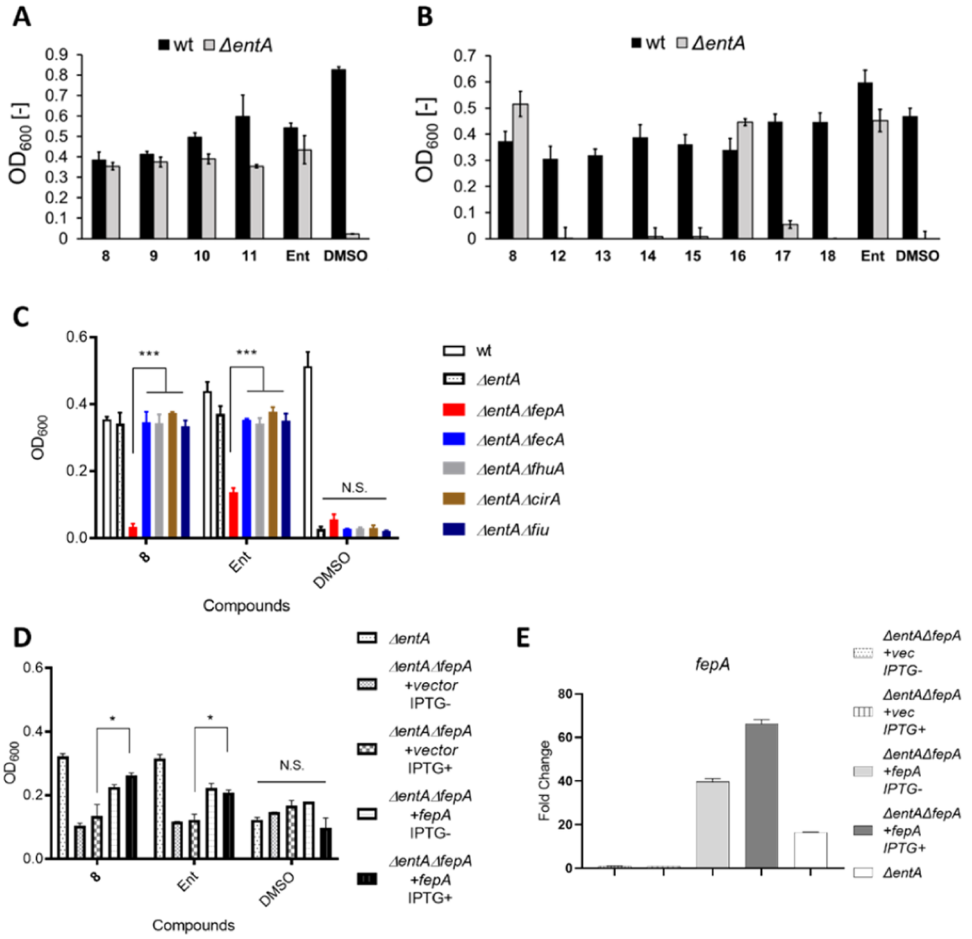

Figure 2. FepA is required for uptake of **8** in *E. coli*. Growth recovery assays with cultures of *E. coli* wt, single- or double-knockout strains that were treated with artificial siderophores, enterobactin, or DMSO and grown under iron-deficient conditions. (A) Treatment with MECAM-based compounds **8**−**11**. (B) Treatment with longer-chain and 1,2,3-substituted analogues **12**−**18**. (C) Treatment of outer membrane receptor-deficient strains with **8**, enterobactin (Ent), or DMSO. (D) Treatment of strains harboring an IPTG-driven *fepA* expression plasmid or a vector control with **8**, enterobactin, or DMSO. (E) RNA expression of *fepA* from cultures in (D) followed by real-time polymerase chain reaction (PCR). Gene expression was normalized against the reference gene *rpoB* and given as relative to Δ*entA*Δ*fepA*+ vec control. Bars represent the means and standard deviations of one representative experiment done in triplicate. Results shown are means and standard deviations of one representative experiment done in triplicate. *$p < 0.05$ and ***$p < 0.001$ (Student's t test). Ent = enterobactin. Vec = vector.

between core moiety and catechol units appears to rather hamper active transport through the outer membrane than impede complex formation. Since the synthesis of MECAM **8** proved to be more convenient than the preparation of the 1,2,3-substituted derivative **16**, we decided to stick to the former in the following studies.

To pinpoint receptors involved in siderophore uptake, growth recovery assays were conducted in double-knockout strains that harbor a gene deletion for one outer membrane receptor and another one for *entA*. The Δ*entA*Δ*fepA* strain showed a growth defect in the presence of the positive control enterobactin (Figure 2C). This demonstrates that *fepA* is a key molecule involved in enterobactin uptake, in line with literature findings.[15] A growth defect was also observed in the Δ*entA*Δ*fepA* strain following treatment with **8**. In contrast, **8** still enabled growth recovery in Δ*entA*Δ*fecA*, Δ*entA*Δ*fhuA*, Δ*entA*Δ*cirA*, and Δ*entA*Δ*fiu* strains (Figure 2C).

To further confirm the role of FepA in **8** uptake, FepA receptors were reintroduced by expressing a plasmid encoding full-length FepA in Δ*entA*Δ*fepA* strain, followed by a growth recovery assay under supplementation of **8** (Figure 2D). The level of *fepA* expression was monitored by real-time PCR (Figure 2E). Complementation of FepA in Δ*entA*Δ*fepA* strain rescued growth under treatment with **8** in iron-limited condition. These results demonstrate that FepA is the essential receptor for uptake of **8**, whereas FecA, FhuA, CirA, and Fiu are dispensable.

MECAM-β-Lactam Conjugate 27 Inhibits the Growth of Multidrug-Resistant Pathogens. For the design of siderophore−antibiotic conjugates, it is crucial to know the main site of subcellular accumulation, to assure a sufficient engagement of the antibiotic target. To measure accumulation, we applied a cell fractionation assay coupled with mass spectrometry detection.[37] Following a growth recovery assay of **10**, the *E. coli* cells from the restored colony were perforated employing an osmotic shock procedure. After releasing the periplasmic fraction *via* centrifugation, an additional sonication step resulted in complete cell lysis, yielding separate membrane and cytoplasmic fractions after centrifugation. Quantifying the content of **10** in these three fractions with mass spectrometry revealed compound enrichment in the membrane and periplasmic fractions, while a low compound concentration was detected in the cytoplasm (Figure 1B).

https://doi.org/10.1021/acs.jmedchem.1c01482
J. Med. Chem. 2021, 64, 15440−15460

Scheme 3. Syntheses of Intermediates 21−23; MECAM−Amino-Penicillin Conjugates 27−30; and Chemical Structures of 24, 31, and the MECAM−Daptomycin Conjugate 32[a]

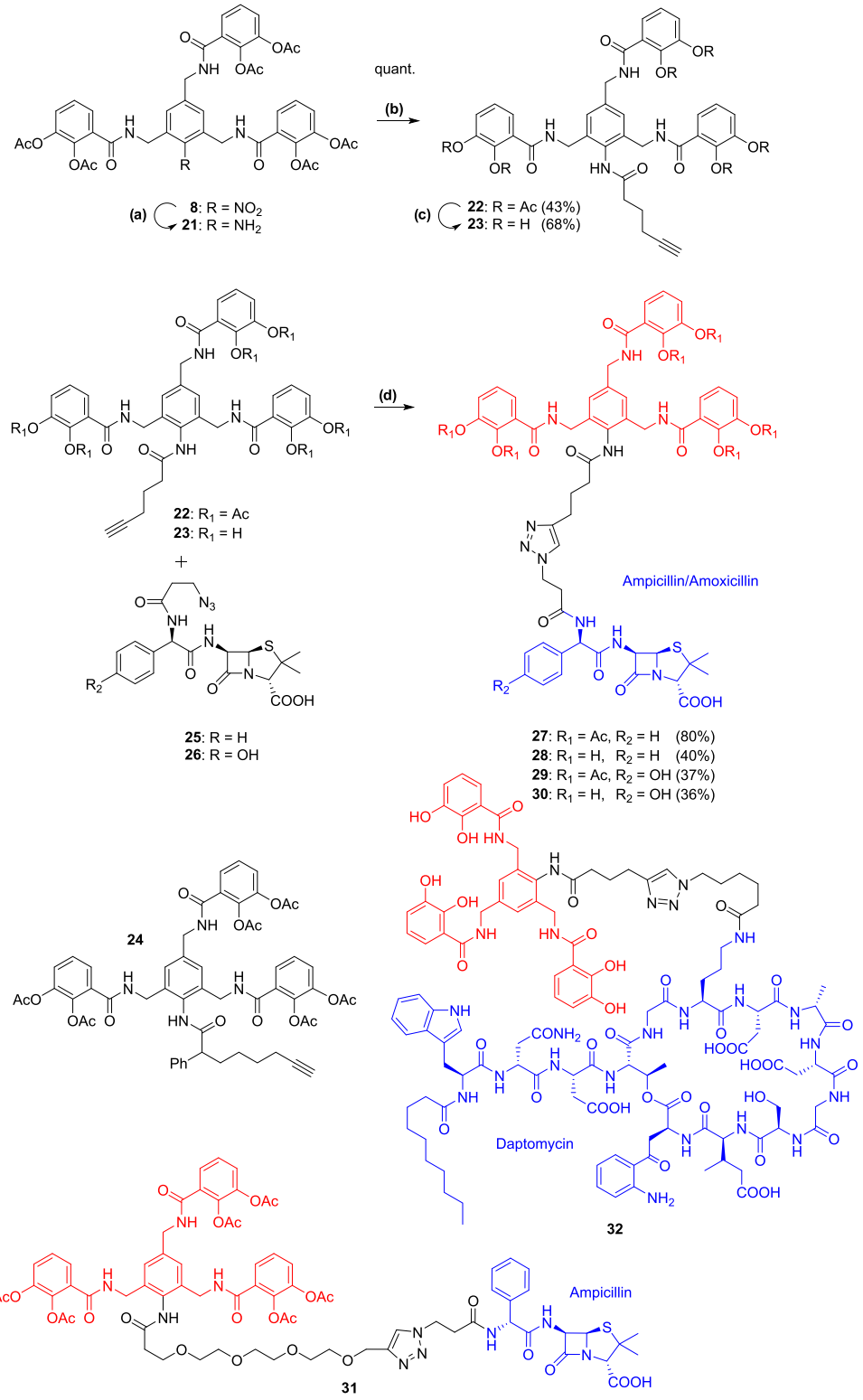

[a]Reagents and conditions: (a) Zn, AcOH, EtOH, THF, 0 °C → rt, 30 min; (b) 5-hexynoic acid, isobutyl chloroformate, NMM, THF, 0 °C → rt, 1 day; (c) NEt_3, MeOH, 0 °C → rt, 2.5 h. (d) $CuSO_4$, sodium ascorbate, (TBTA), H_2O, DMF, rt, 2−3 h. In full conjugates, the antibiotic, linker, and siderophore moieties are labeled in blue, black, and red, respectively.

The findings from the fractionation experiment suggest that antibiotics with periplasmic targets might reach their site of action and were preferably selected for conjugation to the MECAM siderophore. This renders the usage of noncleavable linkers possible, reducing synthetic and stability problems compared to cleavable linkers. The reduction of the nitro

https://doi.org/10.1021/acs.jmedchem.1c01482
J. Med. Chem. 2021, 64, 15440−15460

Table 1. Minimal Inhibitory Concentrations (MICs) of 27−32 against Bacterial Pathogens[a]

strain	27	28	29	30	31	32	amp	amox	cef	dapto
E. coli	≤0.090	0.89 ± 0.0	1.4 ± 0.0	0.87 ± 0.0	0.81 ± 0.48	>64	19 ± 5.4	18 ± 5.2	0.042 ± 0.026	>64
S. aureus	0.12 ± 0.06	5.3 ± 1.6	>46	>56	>64	8.7 ± 3.1	>183	>175	>85	0.36 ± 0.19
A. baumannii	≤0.09	>57	>46	>56	>64	4.4 ± 1.5	>183	>175	0.053 ± 0.029	>39
E. faecium	0.62 ± 0.51	>57	>46	>56	>64	13 ± 0	2.7 ± 1.2	1.3 ± 0.76	>85	0.62−2.5[b]

[a]Ampicillin (amp), amoxicillin (amox), cefiderocol (cef), and daptomycin (dapto) were used as standard antibiotics. [b]Ref 39. MICs (average ± s.d., 3−9 biological replicates) were determined by a curve-fitting procedure and expressed in μM.

group to the aniline **21**, followed by the attachment of a terminal alkyne, gave **22**, which was suitable for subsequent payload installation *via* a copper(I)-catalyzed alkyne-azide cycloaddition (CuAAC). Additionally, the deacetylated congener **23** was also prepared (Scheme 3). To evaluate the extent by which a more sterically demanding linker might affect the ability of MECAM-derived xenosiderophores to translocate ferric iron into Gram-negative bacteria, a phenyl residue branching off close to the core motif was installed to yield **24** (Schemes 3 and S7).

While the artificial siderophores **22** and **23** were functional in the growth recovery assay, growth could not be restored when **24** was applied (Figure S2). Thus, a linear, sterically unhindered linker appears to be necessary to maintain sufficient iron transport characteristics. We next decided to attach the amino-penicillins ampicillin and amoxicillin for the creation of MECAM−antibiotic conjugates, because they address a periplasmic target, and their primary amino groups constitute a viable attachment point according to previous studies.[11] The two amino-penicillins were first equipped with a terminal azide to yield derivatives **25** and **26** (Scheme S8) and then linked to **22** and **23** *via* CuAAC to afford the four MECAM conjugates **27**−**30** (Scheme 3). It is known that replacing an unpolar alkyl linker by a more hydrophilic poly(ethylene glycol) (PEG) linker can have a strong impact on the antibacterial activity of siderophore−drug conjugates.[19] Conjugate **31** comprising a PEG linker was synthesized to compare its activity with the four aforementioned congeners **27**−**30** (Schemes 3 and S9).

Siderophore−antibiotic conjugates **27**−**32** were tested in minimal inhibitory concentration (MIC) assays against bacteria of the so-called ESKAPE panel that comprises the clinically relevant pathogens *S. aureus*, *Klebsiella pneumoniae*, *A. baumannii*, *P. aeruginosa*, *Enterococcus faecium*, and *Enterobacter* sp. To compare conjugated with unconjugated molecules on a molar level, all values are given in μg/mL. Significant inhibition of *K. pneumoniae* and *P. aeruginosa* could not be observed with any conjugate. Conjugates **28**−**31** all prevented growth of *E. coli* at concentrations that were 12- to 24-fold lower than those of unconjugated ampicillin or amoxicillin (Table 1). This result provides a proof of concept that MECAM-based artificial siderophores indeed enhanced the antibiotic activity. However, the spectrum of most conjugates was small: **29**−**31** inhibited only *E. coli*, and **28** was active against *S. aureus* in addition. The efficacy of **31** bearing a PEG linker was substantially lower than that of the corresponding **27** with an alkyl linker against all strains. In fact, **27** was the most potent compound in the panel, as it inhibited the Gram-negative *E. coli* and *A. baumannii* and also the Gram-positive *S. aureus* and *E. faecium* pathogens at nanomolar concentrations. While the enhanced activity of conjugates bearing acetyl-protected catechol moieties is in agreement with previous findings,[24,25] the superiority of ampicillin *vs* amoxicillin in siderophore conjugates is surprising. Compound **27** thereby shows an advantage in comparison with cefiderocol, which is active against Gram-negative bacteria exclusively. In addition, we examined the antibacterial activity of **27** against clinically relevant uropathogenic, enteroaggregative, enteroinvasive, enteropathogenic, and enterotoxigenic *E. coli* strains as well as against Methicillin-resistant *S. aureus* (MRSA), and again found that **27** was at least 8- and 16-fold more potent than free ampicillin in *E. coli* and MRSA, respectively (Table S2).

MECAM−Daptomycin Conjugate 32 Is Active against Multidrug-Resistant Pathogens. To expand the range of antibiotics used in our MECAM conjugates, the lipopeptide daptomycin was selected. Its activity, based on bacterial cell membrane perforation and depolarization, makes it a potent antibiotic against Gram-positive pathogens, whereas it is completely inactive against Gram-negative pathogens due to its large size—unless being actively transported. Thus, representing an ideal test candidate for siderophore transport, daptomycin was derivatized with ε-azido-hexanoic acid at the side chain of its ornithine residue, and subsequently coupled to conjugate **32** (Schemes 3, S10, and S11).

Daptomycin conjugate **32** was less potent against Gram-positive *S. aureus* and *E. faecium* than free daptomycin, and inactive against *E. coli*, *P. aeruginosa*, and *K. pneumoniae*. However, **32** inhibited the growth of *A. baumannii* with an MIC of 4.4 μM, whereas free daptomycin was completely inactive (Table 1). These findings are in line with recent data reported by Miller and co-workers, who demonstrated successful daptomycin transport with *A. baumannii*'s siderophore fimsbactin and artificial congeners.[22,38] Albeit the selectivity for certain bacterial species remains to be understood, it is notable that MECAM-based siderophores mediate the translocation of a very large lipopeptide cargo across the outer membrane.

Uptake of 27 in *E. coli* Depends on Three Receptors. To understand the role of the siderophore uptake pathway for the activity of **27** against *E. coli*, different knockout strains were treated with **27** (Table 2). Strains with single deletions of catecholate receptor genes such as *fepA*, *cirA*, or *fiu* as well as the double-knockout strains Δ*fepA*Δ*cirA*, Δ*fepA*Δ*fiu*, Δ*cirA*Δ*fiu* remained susceptible to **27**. However, the triple knockout of *fepA*, *cirA*, and *fiu* conferred resistance to **27**. Similarly, only a triple knockout of *fepA*, *cirA*, and *fiu* was found to be resistant to cefiderocol,[40] even though a remarkable 64-fold increase in the MIC of cefiderocol was observed in the Δ*cirA*Δ*fiu* strain. Moreover, we examined the influence of downstream components of the catechol siderophore pathway on antimicrobial activities of **27** (Table 2). The outer membrane receptors are coupled to a complex of TonB, ExbB, and ExbD, that provide the energy for active transport.[6] Both **27** and cefiderocol were inactive against a Δ*tonB* strain. Interestingly, a Δ*exbB* strain was fully resistant to **27** but displayed (weakened) sensitivity to cefiderocol (Table

https://doi.org/10.1021/acs.jmedchem.1c01482
J. Med. Chem. 2021, 64, 15440−15460

Table 2. Minimal Inhibitory Concentrations (MICs) of 27 against *E. coli* Wild-Type and Knockout Strains[a]

	MIC (μM)		
strain	27	amp	cef
wt[b]	1.5	46	0.33
Δ*fepA*	2.9	46	0.17
Δ*cirA*	2.9	46	0.66
Δ*fiu*	1.5	46	0.66
Δ*fepA*Δ*cirA*	1.5	46	0.17
Δ*fepA*Δ*fiu*	1.5	46	0.66
Δ*cirA*Δ*fiu*	2.9	46	21
Δ*fepA*Δ*cirA*Δ*fiu*	>12	46	>21
Δ*tonB*	>12	46	>21
Δ*exbB*	>12	46	5.3
Δ*fepB*	2.9	46	0.083
Δ*fepD*	1.5	46	0.083

[a]Ampicillin (amp) and cefiderocol (cef) were used as standard antibiotics. MICs were the minimal concentrations of indicated antibiotics in μM displaying no growth determined by visual inspection. [b]wt = *E. coli* BW25113.

2), indicating that ExbB might play a specific role in **27**-mediated antibacterial activity against *E. coli*. On the other hand, depletion of *fepB*, a periplasmic protein responsible for shutting corresponding cargo from catechol receptors to ABC transporters in the inner membrane,[6] led to a merely 2-fold increase of MIC in **27**. To investigate whether the siderophore import system located at the inner membrane is required, the antibacterial activity of **27** was examined in a Δ*fepD* strain. The Δ*fepD* strain, defective in catechol import from the inner membrane to the cytoplasm, was susceptible to **27**, suggesting that transporting **27** into the periplasm space was sufficient for antibacterial activity. This is in line with the finding that **8** mostly accumulates in the periplasm (Figure 1), and with the fact that the target of ampicillin is located there. In summary, the results suggest that **27** can be taken up by FepA, CirA, and Fiu catechol receptors in *E. coli*; the TonB-coupling of these receptors is essential, whereas the transfer from the periplasm to the cytosol is not.

Truncation of ExbB at Q163 Induces Resistance to 27 in *E. coli*. To investigate the resistance mechanism toward **27** in *E. coli* K-12 BW25113, resistant clones were generated by serial passaging under challenge with **27**. Four clones survived 21 passages and exhibited MICs > 12 μM (Figure 3A). To exclude that the clones became intrinsically drug-resistant, *e.g.*, by overexpressing efflux pumps, they were tested against ampicillin, kanamycin, or cefiderocol, and found to retain sensitivity against those reference antibiotics (Table S3). The genomic DNA of the four clones was isolated, followed by whole-genome sequencing. Mapping the sequences of the parental control and four resistant clones to the reference genome *E. coli* BW25113 (GenBank: CP009273.1) containing 4 631 469 base pairs led to the identification of two single-nucleotide mutations among the four resistant clones (Tables S3 and S4). First, a single-nucleotide mutation observed in all clones was a replacement of guanine to adenine at position 806 in the gene encoding cytochrome bo(3) ubiquinol oxidase subunit I (*cyoB*) (Table S3). This point mutation results in an exchange of glycine to aspartate at position 269 (G269D) in the expressed protein. *cyoABCD* genes encode and form a terminal cytochrome bo oxidase complex that is the main terminal oxidase in the aerobic respiratory chain in *E. coli* and catalyzes the four-electron reduction of molecular oxygen to water.[41,42] Besides, the cytochrome bo terminal oxidase serves as a supplier of PMF, and also CyoB itself was reported to contribute to PMF generation.[42,43] The second nucleotide mutation, found in the first and second clone, incorporated thymine instead of cytosine at position 487 in the gene-biopolymer transport protein exbB, which is a component of the Ton machinery.[44,45] ExbB serves as a supplier of PMF that is required for a conformational change of TonB and the outer membrane receptor to facilitate siderophore uptake.[46,47] The point mutation leads to a stop codon mutation from glutamine (Q163*) of the expressed protein. Both CyoB G269D and ExbB Q163* have not been reported in previous studies.

Given that ExbB forms a complex with TonB to facilitating the siderophore uptake,[45] we examined whether the resistance toward **27** resulted from an impaired siderophore uptake. All resistant clones are able to grow in iron-limited condition (Figure 3B), indicating that the uptake of enterobactin is functional in resistant clones. Moreover, to evaluate whether **27** resistant (**27**^{R}) clones are able to uptake **8**, the *entA* gene was deleted in full-length in all four clones, which were then submitted to growth recovery assays. The growth of Δ*entA*, **27**^{R} clones was recovered upon supplementation with **8** and also with the positive control enterobactin (Figure 3C). This demonstrates that the siderophore uptake system was still functional in **27**^{R} clones. In contrast, double-knockout strains of *entA* and full-length *exbB* showed no growth recovery in the presence of **8**. The fact that neither CyoB G269D nor ExbB Q163* impaired the uptake of enterobactin or **8** demonstrates that the siderophore uptake system in **27**^{R} clones is still functional.

To validate that the CyoB G269D and ExbB Q163* variants were causal for resistance toward **27**, the respective mutated genes were reintroduced by plasmids into Δ*cyoB* and Δ*exbB* strains, respectively. Overexpression of ExbB Q163* in a Δ*exbB* clone was sufficient to confer resistance against **27** up to 12 μM, while strains overexpressing either wild-type ExbB or vector control were susceptible to **27** (Figure 3D,E). The expression efficiency was confirmed by real-time qPCR (Figure 3F). However, reintroducing either wild-type CyoB or CyoB G269D on a plasmid into the Δ*cyoB* strain did not confer resistance to **27** (Figure 3G,H). The complementation efficiency was confirmed by real-time qPCR (Figure 3I). When cultures from **27**^{R} clones no. 3 and 4, carrying only one mutation site in *cyoB*, were further passaged, they returned sensitive to **27**, and the MIC was restored to 1.5 μM (Figure S3). This reverse susceptibility to **27** was not observed in **27**^{R} clones carrying mutations in the *exbB* gene. A further whole-genome sequence analysis (Table S5) confirmed that no additional genetic mutation occurred among those "recovery" clones, *i.e.*, the G269D mutation was still present. In summary, a mutation in ExbB was causal for sustained resistance formation against **27**, whereas the CyoB resistance mutation was transient.

DISCUSSION AND CONCLUSIONS

In this study, we qualified the artificial enterobactin mimic MECAM as a functional and versatile scaffold for siderophore conjugation. The synthesis of a series of MECAM analogues allowed deriving structure−activity relationships, and the structural and electronic properties were calculated by quantum chemistry. Its ferric iron complex was structurally and electronically characterized by quantum-chemically

https://doi.org/10.1021/acs.jmedchem.1c01482
J. Med. Chem. 2021, 64, 15440−15460

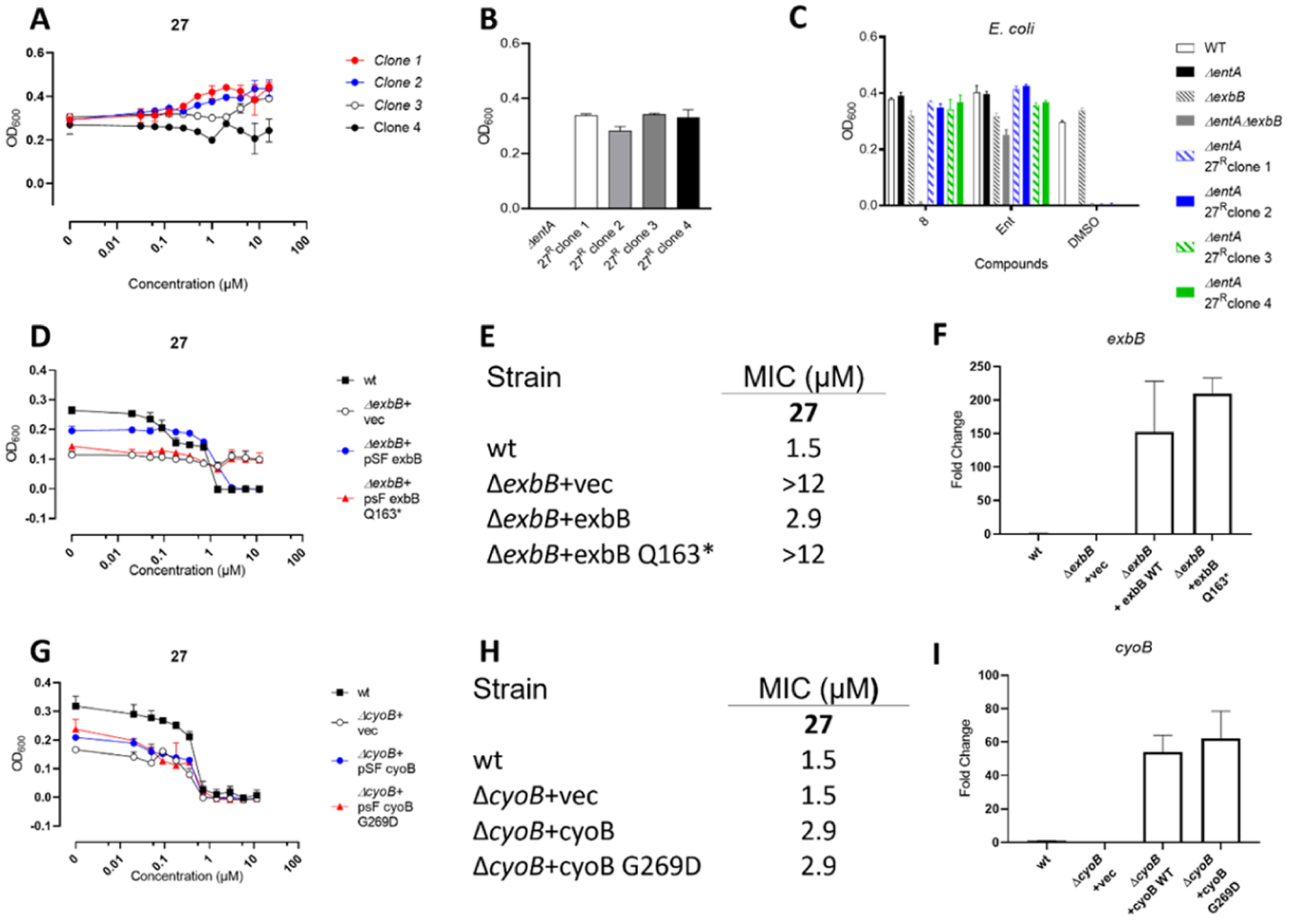

Figure 3. Mechanism of resistance against 27 in *E. coli*. (A) Antibacterial activity of **27** against four 27^R clones was assessed after 24 h treatment in iron-limited MHB. (B, C) Siderophore uptake system is functional in clones resistant to **27**. (B) Growth of Δ*entA* strain and four 27^R clones in LMR medium under iron-limited conditions. (C) Growth recovery of indicated strains treated with **8**, Ent, or DMSO in iron-limited LMR medium for 48 h. (D–I) Overexpression of ExbB163*, but not of CyoB G269D, induces resistance to **27** in *E. coli*. The antibacterial activity of **27** (D) and a summary of MICs (E) against Δ*exbB* strains with a plasmid for the expression of wild-type ExbB, Q163*-truncated ExbB, or with vector control. MIC assays were conducted as mentioned in (A). (F) RNA expression of *exbB* from the cultures shown in (D). Representative results of $n = 2$. The antibacterial activity of **27** (G) and a summary of MICs (H) against Δ*cyoB* strains with a plasmid for the expression of wild-type CyoB, CyoB mutated at G269D, or with vector control. (I) RNA expression of *cyoB* from the cultures shown in (G). Gene expression was normalized against the reference gene *rpoB* and given as relative to wt control. Results shown are means and standard deviations of one representative experiment done in triplicate. Vec: vector control. Ent = enterobactin. Representative results of $n = 3$.

computing structural and energetic properties as well as the relaxed siderophore-Fe(III) force constants (compliance constants) at the DFT level of theory. The prediction of an unprecedented and kinetically stable ferric iron low-spin complex raises the interesting question whether the spin ground state of the iron–siderophore complex might be an additional, hitherto overseen factor in siderophore biology. Notably, spin changes at iron have been highlighted as important for reactivity in the context of iron-mediated oxidation processes.[48] A combination of chemical synthesis, bioanalytical and microbiological assays in the model pathogen *E. coli* led to the selection of the preferred artificial siderophore, and to the conjugation of standard antibiotics. MECAM conjugates led to a potentiation of activity of the β-lactam ampicillin, and they could transport the bulky lipopeptide daptomycin into *A. baumannii*. Compound **27** inhibited the growth of Gram-negative as well as Gram-positive strains at nanomolar concentrations. The enhanced activity of **27** against *S. aureus* cannot be explained by an outer membrane-spanning transporter due to the absence of this membrane. However, siderophore transport into Gram-positive bacteria involves a membrane-anchored binding protein closely located to an ABC transporter that internalizes siderophores.[7] Thus, we hypothesize that conjugate binding to this protein might increase the local β-lactam concentration and thereby the antibacterial potency of the siderophore conjugate compared to free ampicillin.

The dependence of siderophore conjugate uptake on the expression of single receptors that may lead to fast resistance formation, has been an often-mentioned concern.[11,49,50] This study demonstrates that only a triple knockout of three catecholate receptors (FepA, CirA, and Fiu) conferred resistance to **27** in *E. coli* (Table 2), suggesting that **27** is able to use multiple siderophore receptors for its uptake. We hypothesize that the use of artificial siderophores, combining iron binders with a simple core scaffold, may exert advantages with respect to a broader receptor specificity. However, the unconjugated **8** was only transported by FepA (Figure 2),

https://doi.org/10.1021/acs.jmedchem.1c01482
J. Med. Chem. 2021, 64, 15440–15460

which highlights that outer membrane receptors differentiate between compounds **27** and **8**. The observation that TonB and ExbB deletion strains were resistant to **27** implies that Ton-coupled transport indeed plays a key role in the antibacterial activity of **27**.

In addition to experiments with defined knockout strains, we investigated induced resistance upon exposure to **27**, and found a mutation in *exbB*, resulting in a truncated Q163* protein. The causal role of this mutation was proven by the observation that a complementation of ExbB Q163*, but not wild type of ExbB, into a Δ*exbB* strain conferred resistance to **27**. Previous studies showed that ExbB is an integral cytoplasmic membrane (CM) protein with three transmembrane domains.[46,51] It is believed that ExbB has three functions: as a scaffold on stabilizing the structure of Ton machinery, supplier of proton motive force (PMF) for conformational changes of TonB and the associated outer membrane receptor, and signal transduction.[46,47] ExbB Q163* is a truncated form of ExbB lacking the third transmembrane domain (TMD3) and the cytoplasmic carboxy terminus. By site-directed mutagenesis, Baker et al. found key residues located in the three TMDs of ExbB and proposed that TMD 1 mainly interacts with the TMD of TonB, TMD 2 interacts with ExbD, whereas TMD 3 is involved in signal transduction. The fact that resistant clones with ExbB Q163* mutation were able to take up either enterobactin or **8** (Figure 3) suggests that the truncated form of ExbB Q163* is not essential for siderophore uptake in general but specifically mediates entry of **27** into *E. coli*. While the mechanism behind this is not understood, the finding again highlights that "free" and conjugated siderophore mimics behave differently.

The protein CyoB (cytochrome bo(3) ubiquinol oxidase subunit I) functions as the major terminal oxidase in the aerobic respiratory chain of *E. coli* and contributes to PMF generation.[52,53] However, the reintroduction of CyoB G269D into a Δ*cyoB* strain did not lead to a restoration of resistance to **27** (Figure 3). Besides, cultures from $\mathbf{27^R}$ clones with only one mutation site in *cyoB* returned sensitive to **27** after a few (MIC = 1.45 μM) passages (Table S5). This transient resistance allows bacteria to temporarily survive upon antibiotic exposure.[54] A previous study from Lázár et al. revealed that mutations of CyoB contribute to aminoglycoside resistance *via* the reduction of PMF in the presence of other mutations in other genes.[55] Considering that CyoB G269D mutation existed in all $\mathbf{27^R}$ clones, CyoB G269D might impede the uptake of **27** by reducing the membrane potential as well as PMF, even though a CyoB G269D alone is not sufficient for sustained resistance to **27**. Thus, the formation of ExbB163*, but not CyoB G269D, played an essential role in resistance formation in *E. coli*. While previous resistance studies focused mainly on outer membrane receptors for siderophores, this work highlights the importance of additional components, albeit also related to uptake to the periplasm. In contrast, downstream transport into the cytoplasm was not relevant, in line with the antibiotic mechanism of **27**.

In summary, the data qualify the versatile MECAM scaffold as a transporter of antibiotic cargo, and they highlight the potential of artificial siderophores as "Trojan Horses" to fight multidrug-resistant bacteria.

EXPERIMENTAL SECTION

General Chemistry Methods. Commercially obtained chemicals were used without any further purification. All organic solvents possessed HPLC-grade purity. Dried solvents were used unless water was part of the solvent mixture or the total amount of solvent in the reaction was bigger than 30 mL. Dichloromethane was dried over molecular sieves (4 Å). All other dried solvents were purchased in a water-free form. Reactions requiring dried solvents were conducted in twofold baked-out glassware under a nitrogen atmosphere. Removal of organic solvents was conducted on rotational evaporators at 30 °C. For the removal of water, a temperature of 40 °C was applied. Lyophilization of compounds was conducted on an α 2−4 LSCbasic (Christ) lyophilizer after freezing compound solutions in liquid nitrogen. Centrifugations were performed on a Universal 32 R (Hettich) centrifuge. Absolute reaction yields are given only after the neat compound was analyzed by NMR spectroscopy. Yields of unpurified compounds were only calculated to allow stoichiometric calculations for the next synthetic step. In these cases, absolute overall yields are given with the final step of the respective synthesis. All compounds had purities ≥95% as determined by high-performance liquid chromatography (UV detection) and $^1H/^{13}C$ NMR analysis.

Synthetic Procedures. *Compound* ***5***. To a solution of 2,3-dihydroxybenzoic acid (**4**, 4.00 g, 26.0 mmol, 1 equiv) and 4-(dimethylamino)-pyridine (318 mg, 2.60 mmol, 0.1 equiv), acetic anhydride (7.37 mL, 7.96 g, 77.9 mmol, 3 equiv) and triethylamine (21.6 mL, 15.8 g, 156 mmol, 6 equiv) were added. The reaction mixture was refluxed for 3 h, cooled to rt, and the solvent was removed. The residue was washed with cold hydrochloric acid (0.5 M) and cold saturated sodium chloride solution (2 × 75 mL each) and dried over sodium sulfate. After removing the solvent and drying *in vacuo*, **5** was obtained as a brownish solid (5.27 g, 22.1 mmol, 85%) and used for the preparation of **6** without further purification.

Compound ***6***. Oxalyl chloride (566 μL, 838 mg, 6.6 mmol, 2 equiv) was added dropwise to a solution of **5** (786 mg, 3.30 mmol, 1 equiv) in dichloromethane (20 mL) and dimethylformamide (200 μL) over a time of 5 min at 0 °C. The reaction was stirred for 10 min at 0 °C, warmed to rt, and stirred for 2.5 h. After removing the solvent, crude product **6** was dried *in vacuo* overnight and used in subsequent reactions without further purification.

Compound ***8a***. Tris(bromomethyl)benzene (**7**, 1.67 g, 4.68 mmol) was added in small portions to a mixture of nitric acid (65%) and concentrated sulfuric acid (10 mL each) at 0 °C. The reaction mixture was warmed to rt, stirred for 1 day, poured on ice, and extracted with ethyl acetate (2 × 25 mL). The combined organic layers were washed with saturated solutions of sodium hydrogen carbonate and sodium chloride (2 × 30 mL each) and dried over sodium sulfate. After removing the solvent and drying *in vacuo*, **7a** was obtained as a light yellow solid (1.72 g, 4.28 mmol, 91%) and used in subsequent reactions without further purification.

Compound ***8***. An aqueous solution of ammonia (30%, 10 mL) was added dropwise to a solution of **8a** (402 mg, 1.00 mmol, 1 equiv) in tetrahydrofuran and ethanol (5 mL each). The reaction mixture was stirred overnight. After removing the solvent and drying *in vacuo*, the residue was dissolved in aqueous sodium hydrogen carbonate solution (0.5 M, 20 mL). Compound **6** (3.3 mmol, 3.3 equiv) in 1,4-Dioxane (20 mL) was added to this solution at 0 °C over a time of 15 min. The reaction mixture was warmed to rt, mixed with ice, and extracted with ethyl acetate (3 × 30 mL). The combined organic layers were washed with saturated solutions of sodium hydrogen carbonate and sodium chloride (2 × 75 mL each) and dried over sodium sulfate. After removing the solvent, **8** was obtained by purification *via* automatic flash chromatography (CH_2Cl_2/MeOH) as a light yellow solid (510 mg, 586 μmol, 59% over 3 steps).

TLC R_f = 0.21 (CH_2Cl_2/MeOH = 20:1).

^1H NMR (700 MHz, DMSO-d_6): δ [ppm] = 2.17 (s, 3H), 2.19 (s, 6H), 2.28 (s, 3H), 2.29 (s, 6H), 4.42 (d, *J* = 5.7 Hz, 4H), 4.46 (d, *J* = 5.7 Hz, 2H), 7.25 (t, *J* = 7.9 Hz, 1H), 7.32(t, *J* = 7.9 Hz, 2H), 7.37 (dd, *J* = 8.1, 1.4 Hz, 1H), 7.39 (dd, *J* = 8.1, 1.5 Hz, 2H), 7.41 (s, 2H), 7.46 (dd, *J* = 7.8, 1.5 Hz, 1H), 7.48 (dd, *J* = 7.7, 1.5 Hz, 2H),9.02 (t, *J* = 5.8 Hz, 2H), 9.06 (t, *J* = 6.0 Hz, 1H).

^{13}C NMR (176 MHz, DMSO-d_6): δ [ppm] = 20.2, 20.3, 38.8, 42.0, 125.6, 125.8, 126.0, 126.1, 126.2, 126.3, 130.1, 130.3, 131.4, 140.2, 140.2, 142.7, 142.8, 147.0, 164.8, 164.8, 167.9, 167.9, 168.3.

https://doi.org/10.1021/acs.jmedchem.1c01482
J. Med. Chem. 2021, 64, 15440−15460

$C_{42}H_{38}N_4O_{17}$ (870.78), exact mass: 870.2232.

ESI-HRMS (m/z): $[M + Na]^+$ calcd for $C_{42}H_{38}N_4NaO_{17}$: 893.2130; found: 893.2119.

Compound ***9***. An aqueous solution of ammonia (30%, 2.4 mL) was added dropwise to a solution of 1,3,5-tris(bromomethyl)benzene (**7**, 89.0 mg, 250 μmol, 1 equiv) in tetrahydrofuran and ethanol (1.2 mL each). The reaction mixture was stirred for 2.5 h and the resulting precipitate was filtered off. After removing the solvent and drying *in vacuo*, the residue was dissolved in aqueous sodium hydrogen carbonate solution (0.5 M, 5 mL). Compound **6** (875 μmol, 3.5 equiv) in 1,4-Dioxane (4 mL) was added to this solution at 0 °C. The reaction mixture was stirred at 0 °C for 5 min, mixed with ice, and extracted with ethyl acetate (3 × 10 mL). The combined organic layers were washed with saturated sodium chloride solution (2 × 20 mL) and dried over sodium sulfate. After removing the solvent, **9** was obtained by purification *via* HPLC as a white solid (23.4 mg, 28.3 μmol, 11% over 2 steps).

^{1}H NMR (500 MHz, DMSO-d_6): δ [ppm] = 2.17 (s, 9H), 2.28 (s, 9H), 4.39 (d, J = 5.9 Hz, 6H), 71.5 (s, 3H), 7.32 (t, J = 7.9 Hz, 3H), 7.37 (dd, J = 8.1, 1.7 Hz, 3H), 7.49 (dd, J = 7.6, 1.7 Hz, 3H), 8.94 (t, J = 6.0 Hz, 3H).

^{13}C NMR (125 MHz, DMSO-d_6): δ [ppm] = 20.2, 20.3, 42.4, 124.5, 125.4, 126.0, 126.3, 130.8, 139.5, 140.1, 142.8, 164.5, 167.9, 168.3.

$C_{42}H_{39}N_3O_{15}$ (825.78), exact mass: 825.2381.

ESI-HRMS (m/z): $[M + H]^+$ calcd for $C_{42}H_{40}N_3O_{15}$: 826.2459; found: 826.2453.

Compound ***10***. Compound **8** (26.1 mg, 30.0 μmol) was stirred in aqueous potassium hydroxide solution (1 M, 15 mL) for 1 h. The reaction mixture was acidified with hydrochloric acid (1 M) and extracted with ethyl acetate (25 mL). The combined organic layer was decanted and dried over sodium sulfate. After removing the solvent, **10** was obtained by purification *via* HPLC as a white solid (9.0 mg, 14.5 μmol, 48%).

^{1}H NMR (500 MHz, DMSO-d_6): δ [ppm] 4.50 (d, J = 5.5 Hz, 6H), 6.63 (t, J = 7.9 Hz, 1H), 6.68 (t, J = 8.0 Hz, 2H), 6.89-−6.95 (m, 3H), 7.21 (dd, J = 8.2, 1.3 Hz, 1H), 7.25 (dd, J = 8.2, 1.3 Hz, 2H), 7.44 (s, 2H), 9.14 (s_{br}, 1H), 9.21 (s_{br}, 2H), 9.33 (t, J = 5.7 Hz, 2H), 9.39 (t, J = 6.0 Hz, 1H) 12.15 (s_{br}, 2H), 12.37 (s_{br}, 1H).

^{13}C NMR (125 MHz, DMSO-d_6): δ [ppm] = 38.6, 41.9, 114.9, 115.0, 117.2, 117.5, 118.0, 118.2, 118.9, 119.0, 126.5, 131.5, 142.6, 146.1, 147.2, 149.2, 149.5, 169.8, 169.9.

$C_{30}H_{26}N_4O_{11}$ (618.56), exact mass: 618.1598.

ESI-HRMS (m/z): $[M + H]^+$ calcd for $C_{30}H_{27}N_4O_{11}$: 641.1496; found: 641.1509.

Compound ***11***. Compound **9** (4.12 mg, 5.00 μmol) was stirred in aqueous potassium hydroxide solution (1 M, 2 mL) for 90 min. The reaction mixture was acidified with hydrochloric acid (2 M) and extracted with ethyl acetate (3 × 5 mL). The combined organic layers were dried over sodium sulfate. After removing the solvent, **11** was obtained by purification *via* HPLC as a white solid (1.20 mg, 2.08 μmol, 42%).

^{1}H NMR (500 MHz, DMSO-d_6): δ [ppm] = 4.46 (d, J = 8.2 Hz, 6H), 6.67 (t, J = 8.0 Hz, 3H), 6.91 (dd, J = 7.8, 1.3 Hz, 3H), 7.19, (s, 3H), 7.29 (dd, J = 8.2, 1.3 Hz, 3H), 9.14 (s_{br}, 3H), 9.34 (t, J = 6.0 Hz, 3H), 12.63 (s, 3H).

^{13}C NMR (125 MHz, DMSO-d_6): δ [ppm] = 42.3, 114.9, 117.2, 118.0, 118.9, 124.9, 139.4, 146.2, 149.7, 169.7.

$C_{30}H_{27}N_3O_9$ (573.56), exact mass: 573.1747.

ESI-HRMS (m/z): $[M + H]^+$ calcd for $C_{30}H_{28}N_3O_9$: 574.1826; found: 574.1819.

Compound ***12a***. Sodium cyanide (2.18 g, 43.2 mmol, 12 equiv), a saturated solution of sodium hydrogen carbonate (10 mL), and water (10 mL) were added to a solution of tris(bromomethyl)benzene (1.28 g, 3.60 mmol, 1 equiv) in tetrahydrofuran (10 mL). The solution was stirred for 3 h, and hydrochloric acid (1 M, *ca.* 38 mL) was carefully added *via* a droplet funnel until a pH of 6 was reached. The solution was stirred for 2 h and the resulting precipitate was removed *via* centrifugation, taken up in acetonitrile. The solution was dried over sodium sulfate. After removing the solvent and drying *in vacuo*, **12a** was obtained as a light yellow solid (630 mg, 3.23 mmol, 90%) and used for the synthesis of **12b** without further purification.

Compound ***12b***. To a solution of potassium hydroxide (25%) in water (8 mL) and ethanol (4 mL), **12a** (605 mg, 3.10 mmol) was added. This solution was heated to 100 °C in a sealed glass vial and stirred overnight. The solution was poured on ice water (*ca.* 100 mL) and acidified to pH ≈ 1 with hydrochloric acid (6 M). After the addition of saturated sodium chloride solution, the mixture was extracted with ethyl acetate (5 × 50 mL) and the combined organic layers were dried over sodium sulfate. After removing the solvent and drying *in vacuo*, **12b** was obtained as a light yellow solid (700 mg, 2.78 mmol, 90%) and used for the synthesis of **12c** without further purification.

Compound ***12c***. A solution of **12b** (698 mg, 2.77 mmol, 1 equiv), trimethyl orthoformate (909 μmol, 882 mg, 8.31 mmol, 3.3 equiv), and a few drops of concentrated sulfuric acid in methanol (16 mL) was heated to 72 °C in a sealed glass vial and stirred for 18 h. After removing the solvent, the residue was taken up in ethyl acetate (25 mL). The organic layer was washed with saturated solutions of sodium hydrogen carbonate and sodium chloride (2 × 25 mL each) and dried over sodium sulfate. After removing the solvent and drying *in vacuo*, **12c** was obtained as a light yellow oil (708 mg, 2.41 mmol, 87%) and used for the synthesis of **12d** without further purification.

Compound ***12d***. Lithium aluminum hydride (369 mg, 9.72 mmol, 4.5 equiv) was added to a solution of **12c** (635 mg, 2.16 mmol, 1 equiv) in tetrahydrofuran (10 mL). The reaction mixture was stirred for 4 h, carefully quenched with a saturated solution of potassium sodium tartrate, and filtered over a celite frit. The filter cake was repeatedly washed with diethyl ether and methanol and the combined organic layers were dried over sodium sulfate. After removing the solvent, **12d** was obtained by purification *via* flash chromatography (CH_2Cl_2/MeOH 20:1 → 15:1 → 10:1) as a white solid (190 mg, 904 μmol, 30% over four steps)

TLC R_f = 0.15 (CH_2Cl_2/MeOH = 20:1).

^{1}H NMR (500 MHz, methanol-d_4): δ [ppm] = 2.77 (t, J = 7.0 Hz, 6H), 3.74 (t, J = 7.0 Hz, 6H), 6.94 (s, 3H).

^{13}C NMR (125 MHz, methanol-d_4): δ [ppm] = 40.4, 64.4, 128.8, 140.5.

$C_{12}H_{18}O_3$ (210.27), exact mass: 210.1256.

ESI-HRMS (m/z): $[M + Na]^+$ calcd for $C_{12}H_{18}NaO_3$: 233.1154; found: 233.1148.

Compound ***12e***. A solution of **12d** (174 mg, 828 μmol) in hydrobromic acid (45%, 10 mL) was heated to 125 °C in a sealed glass vial, stirred for 5 h, and stirred overnight while slowly cooling to rt. The solution was poured on ice and extracted with ethyl acetate (3 × 40 mL). The combined organic layers were washed with saturated solutions of sodium hydrogen carbonate and sodium chloride (2 × 50 mL each) and dried over sodium sulfate. After removing the solvent, **12e** was obtained by purification *via* flash chromatography (PE/EA 100:1 → 50:1) as a white solid (237 mg, 594 μmol, 72%)

TLC R_f = 0.46 (PE/EA = 20:1).

^{1}H NMR (500 MHz, $CDCl_3$): δ [ppm] = 3.15 (t, J = 7.6 Hz, 6H), 3.57 (t, J = 7.6 Hz, 6H), 6.97 (s, 3H).

^{13}C NMR (125 MHz, $CDCl_3$): δ [ppm] = 32.7, 39.1, 127.6, 139.6.

Compound ***12f***. Compound **12e** (39.9 mg, 100 μmol) was added to a vigorously stirred mixture of nitric acid (65%, 500 μL) and concentrated sulfuric acid (1 mL) in small portions at 0 °C. The reaction mixture was stirred for 2 h at 0 °C and quenched with ice water. The mixture was extracted with ethyl acetate (2 × 10 mL). The combined organic layers were washed with saturated solutions of sodium hydrogen carbonate and sodium chloride (2 × 20 mL each) and dried over sodium sulfate. After removing the solvent, **12f** was obtained by purification *via* flash chromatography (PE/EA 20:1 → 15:1) as a white solid (12.2 mg, 27.5 μmol, 28%)

TLC R_f = 0.21 (PE/EA = 20:1).

^{1}H NMR (500 MHz, $CDCl_3$): δ [ppm] = 3.14 (t, J = 7.3 Hz, 4H), 3.23 (t, J = 7.1 Hz, 2H), 3.58 (t, J = 7.3 Hz, 4H), 3.60 (t, J = 7.3 Hz, 2H), 7.29 (s, 2H).

^{13}C NMR (125 MHz, $CDCl_3$): δ [ppm] = 31.0, 31.8, 34.9, 38.4,130.5, 131.1141.6, 150.0.

https://doi.org/10.1021/acs.jmedchem.1c01482
J. Med. Chem. 2021, 64, 15440−15460

Compound ***12***. An aqueous solution of ammonia (30%, 300 μL) was added dropwise to a solution of **12f** (12.0 mg, 27.0 μmol, 1 equiv) in tetrahydrofuran and ethanol (150 μL each). The reaction mixture was heated to 90 °C in a sealed glass vial and stirred overnight. After removing the solvent and drying *in vacuo*, the residue was dissolved in aqueous sodium hydrogen carbonate solution (0.5 M, 750 μL). Compound **6** (108 μmol, 4 equiv) in 1,4-dioxane (500 μL) was added to this solution dropwise at 0 °C. The reaction mixture was warmed to rt, stirred for 15 min, mixed with ice, and extracted with ethyl acetate (3 × 5 mL). The combined organic layers were dried over sodium sulfate. After removing the solvent, **12** was obtained by purification *via* HPLC as a white solid (5.50 mg, 6.03 μmol, 22% over 2 steps).

^{1}H NMR (700 MHz, DMSO-d_6): δ [ppm] = 2.19 (s, 3H), 2.19 (s, 6H), 2.27 (s, 3H), 2.28 (s, 6H), 2.74 (t, J = 7.4 Hz, 4H), 2.85 (t, J = 7.1 Hz, 2H), 3.42 (dd, J = 13.8, 6.7 Hz, 4H), 4.46 (dd, J = 13.3, 6.9 Hz, 2H), 7.27 (s, 2H), 7.34−7.40(m, 7H), 7.40−7.44 (m, 2H), 8.45 (t, J = 5.6 Hz, 1H), 8.52 (t, J = 5.6 Hz, 2H).

^{13}C NMR (176 MHz, DMSO-d_6): δ [ppm] = 20.1, 20.2, 20.3, 30.3, 34.4, 39.6, 40.1, 125.3, 125.4, 125.9, 125.9, 126.2, 129.3, 130.3, 130.8, 131.0. 140.0, 140.0, 142.2, 142.8, 149.8, 164.6, 164.6, 167.7, 168.3.

$C_{45}H_{44}N_4O_{17}$ (912.86), exact mass: 912.2701.

ESI-HRMS (m/z): $[M + H]^+$ calcd for $C_{45}H_{45}N_4O_{17}$: 913.2780; found: 913.2774.

Compound ***13a***. Triethyl phosphonoacetate (2.28 g, 10.2 mmol, 3.3 equiv) was added to a mixture of sodium hydride (60% in mineral oil, 432 mg, 10.8 mmol, 3.5 equiv) in tetrahydrofuran (24 mL) min at 0 °C over a time of 15 with a syringe pump. The reaction mixture was warmed to rt and stirred for 30 min. 1,3,5-Triformyl benzene (500 mg, 3.08 mmol, 1 equiv) in tetrahydrofuran (6 mL) was added at 0 °C, and the reaction mixture was sonicated for 10 min, stirred overnight at rt and quenched with 2-propanol and ice. After removing the solvent, the residue was taken up in dichloromethane (25 mL) and hydrochloric acid (1 M, 25 mL). After separating the phases, the aqueous layer was extracted with dichloromethane (25 mL) and the combined organic layers were washed with water and a saturated solution of sodium chloride (2 × 40 mL each) and dried over sodium sulfate. After removing the solvent and drying *in vacuo*, **13a** (1.05 g, 2.82 mmol, 92%) was obtained and used for the synthesis of **13b** without further purification.

Compound ***13b***. A solution of **13a** (1.05 g, 2.82 mmol) in methanol (30 mL) was flushed with nitrogen for 10 min. Palladium on charcoal (10%, 105 mg) was added and the reaction mixture was flushed with hydrogen for 10 min, stirred under a hydrogen atmosphere for 16 h, and filtered over a celite frit. The filter cake was washed with methanol and the filtrate was dried over sodium sulfate. After removing the solvent and drying *in vacuo*, **13b** (1.02 g, 2.70 mmol, 96%) was obtained and used for the synthesis of **13c** without further purification.

Compound ***13c***. Compound **13b** (1.02 g, 2.70 mmol, 1 equiv) in tetrahydrofuran (10 mL) was added to a mixture of lithium aluminum hydride (307 mg, 8.10 mmol, 3 equiv) in tetrahydrofuran (10 mL) at 0 °C over a time of 30 min with a syringe pump. The reaction mixture was warmed to rt, quenched with hydrochloric acid (1 M, 20 mL) at 0 °C, and filtered over a celite frit. The solution was extracted with dichloromethane (4 × 20 mL) and the combined organic layers were dried over sodium sulfate. After removing the solvent and drying *in vacuo*, **13c** (438 mg, 1.74 mmol, 64%) was obtained and used for the synthesis of **13d** without further purification.

Compound ***13d***. Triphenylphosphine dibromide (4.40 g, 10.4 mmol, 6 equiv) was added to a vigorously stirred solution of **13c** (438 mg, 1.74 mmol, 1 equiv) in dichloromethane (10 mL). The solution was stirred overnight and the solvent was removed. The residue was taken up in petrol ether (75 mL) vigorously stirred for 30 min. The precipitate was removed *via* centrifugation. After removing the solvent and drying *in vacuo*, **13d** (319 mg, 723 μmol, 23% over 4 steps) was obtained by purification *via* flash chromatography (PE/EA 50:1) as a colorless oil.

TLC R_f = 0.32 (PE/EA = 50:1).

^{1}H NMR (500 MHz, $CDCl_3$): δ [ppm] = 2.14−2.21 (m, 6H), 2.72−2.78 (m, 6H), 3.42 (t, 6.6 Hz, 6H), 6.91 (s, 3H).

^{13}C NMR (125 MHz, $CDCl_3$): δ [ppm] = 33.1, 33.8, 34.1, 126.6, 140.9.

Compound ***13e***. Compound **13d** (44.1 mg, 100 μmol) was added to a vigorously stirred mixture of nitric acid (50%, 500 μL) and concentrated sulfuric acid (500 μL) in small portions at 0 °C. The reaction mixture was stirred for 11 h at 0 °C and for 4.5 h at rt and poured on ice water. The mixture was extracted with ethyl acetate (2 × 10 mL). The combined organic layers were washed with saturated solutions of sodium hydrogen carbonate and sodium chloride (2 × 15 mL each) and dried over sodium sulfate. After removing the solvent and drying *in vacuo*, **13e** (29.0 mg, 59.7 mmol, 60%) was obtained and used for the synthesis of **13f** without further purification.

Compound ***13***. An aqueous solution of ammonia (30%, 1 mL) was added dropwise to a solution of **13e** (29.0 mg, 59.7 μmol, 1 equiv) in tetrahydrofuran (500 μL) and ethanol (100 μL). The reaction mixture was heated to 90 °C in a sealed glass vial and stirred overnight. After removing the solvent and drying *in vacuo*, the residue was dissolved in aqueous sodium hydrogen carbonate solution (0.5 M, 2 mL). Compound **6** (209 μmol, 3.5 equiv) in 1,4-dioxane (2 mL) was added to this solution dropwise at 0 °C. The reaction mixture was stirred for 5 min at 0 °C and for 10 min at rt, mixed with ice, and extracted with ethyl acetate (3 × 8 mL). The combined organic layers were washed with saturated solutions of sodium hydrogen carbonate and sodium chloride (2 × 15 mL each) and dried over sodium sulfate. After removing the solvent, **13** was obtained by purification *via* HPLC as a white solid (14.0 mg, 14.7 μmol, 15% over 3 steps).

^{1}H NMR (700 MHz, DMSO-d_6): δ [ppm] = 1.72−1.78 (m, 4H), 1.78−1.83 (m, 2H),2.21 (s, 9H), 2.29 (s, 9H), 2.52−2.56 (m, 4H), 2.64−2.68 (m, 2H),3.19−3.24 (m, 6H), 7.24 (s, 2H), 7.34−7.39 (m, 6H), 7.41−7.45 (m, 3H), 8.41−8.47 (m, 3H).

^{13}C NMR (176 MHz, DMSO-d_6): δ [ppm] = 20.2, 20.2, 20.3, 28.1, 30.2, 30.4, 32.1, 38.5, 38.6, 125.3, 125.9, 125.9, 126.2, 128.2, 131.2, 131.2, 132.7, 139.9, 140.0, 142.8, 144.7, 149.1, 164.6, 167.7, 167.8, 168.3.

$C_{48}H_{50}N_4O_{17}$ (954.94), exact mass: 954.3171.

ESI-HRMS (m/z): $[M + Na]^+$ calcd for $C_{48}H_{50}N_4NaO_{17}$: 977.3069; found: 977.3063.

2-Nitrobenzene-1,3,5-tricarboxylic Acid. Potassium permanganate (23.7 g, 150 mmol, 10 equiv) was added to a solution of 2-nitromesitylene (2.48 g, 15 mmol, 1 equiv), sodium hydrogen carbonate (5.04 g, 60 mmol, equiv), and Aliquat 336 (0.5 mL) in water (80 mL) over a time of 15 min in small portions. The reaction mixture was refluxed for 3 days and filtered over a celite pad. The filtrate was acidified with concentrated hydrochloric acid (20 mL) and extracted with diethyl ether (5 × 100 mL). The combined organic layers were dried over sodium sulfate. After removing the solvent and drying *in vacuo*, 2-nitrobenzene-1,3,5-tricarboxylic acid was obtained as a white solid (834 mg, 3.27 mmol, 22%).

^{1}H NMR (500 MHz, DMSO-d_6): δ [ppm] = 8.61 (s, 2H), 14.01 (s_{br}, 1H).

^{13}C NMR (125 MHz, DMSO-d_6): δ [ppm] = 125.2, 132.9, 135.2, 150.6, 163.3, 164.5.

Compound ***14a***. EDCI (61.3 mg, 320 μmol, 3.2 equiv) and HOBt (43.2 mg, 32.0 mmol, 3.2 equiv) were added to a solution of 2-nitrobenzene-1,3,5-tricarboxylic acid (25.5 mg, 100 μmol, 1 equiv) and diisopropylamine (87.0 μL, 64.6 mg, 500 μmol, 5 equiv) in dimethylformamide (2 mL). The solution was stirred for 1 h at 0 °C, and *tert*-butyl *N*-(2-aminoethyl)carbamate (52.9 mg, 330 μmol, 3.3 equiv) was added dropwise. The solution was stirred overnight at rt, quenched with water, and extracted with ethyl acetate (3 × 5 mL). The combined organic layers were washed with hydrochloric acid (1 M, 10 mL), saturated sodium hydrogen carbonate solution (10 mL), and saturated sodium chloride solution (3 × 10 mL). After removing the solvent and drying *in vacuo*, **14a** was obtained and used for the synthesis of **14** without further purification.

Compound ***14***. Trifluoroacetic acid (1 mL) was added to a solution of **14a** (100 μmol, 1 equiv) in dichloromethane (3 mL) at 0 °C over a time of 15 min with a syringe pump. The solution was

https://doi.org/10.1021/acs.jmedchem.1c01482
J. Med. Chem. 2021, 64, 15440−15460

stirred for 30 min at 0 °C and for 30 min at rt. After the addition of toluene (4 mL), the solvent was removed and the residue was dried *in vacuo*. The residue was dissolved in aqueous sodium hydrogen carbonate solution (0.5 M, 4 mL). Compound **6** (400 μmol, 4 equiv) in 1,4-dioxane (4 mL) was added to this solution at 0 °C over a time of 15 min. The reaction mixture was stirred at 0 °C for 5 min, warmed to rt, mixed with ice, and extracted with ethyl acetate (3 × 5 mL). The combined organic layers were washed with saturated solutions of sodium hydrogen carbonate and sodium chloride (2 × 10 mL each) and dried over sodium sulfate. After removing the solvent, **14** was obtained by purification *via* HPLC as a white solid (9.90 mg, 9.50 μmol, 10% over three steps).

^{1}H NMR (700 MHz, DMSO-d_6): δ [ppm] = 2.20 (s, 3H), 2.23, (s, 6H), 2.28 (s, 3H), 2.28 (s, 6H), 3.36 (s_{br}, 8H), 3.39 (dd, J = 12.8, 6.4 Hz, 2H), 3.45 (dd, J = 12.6, 6.2 Hz, 2H), 7.35−7.39 (m, 6H), 7.49−7.53 (m, 3H), 8.22 (s, 2H), 8.48 (t, J = 5.4 Hz, 2H), 8.50 (t, J = 5.7 Hz, 1H), 8.86 (t, J = 5.6 Hz, 1H), 9.00 (t, J = 5.2 Hz, 2H),

^{13}C NMR (176 MHz, DMSO-d_6): δ [ppm] = 20.2, 20.2, 20.3, 38.5, 38.6, 38.8, 39.1, 125.5, 125.5, 126.1, 126.1, 126.2, 126.2, 128.9, 130.7, 130.8, 131.1, 136.5, 140.1, 140.1, 142.8, 142.9, 147.9, 164.0, 164.0, 164.8, 167.8, 168.3, 168.3.

$C_{48}H_{47}N_7O_{20}$ (1041.93), exact mass: 1041.2876.

ESI-HRMS (m/z): $[M + H]^+$ calcd for $C_{48}H_{48}N_7O_{20}$: 1042.2954; found: 1042.2958.

Compound ***15a***. EDCI (61.3 mg, 320 μmol, 3.2 equiv) and HOBt (43.2 mg, 32.0 mmol, 3.2 equiv) were added to a solution of 2-nitrobenzene-1,3,5-tricarboxylic acid (25.5 mg, 100 μmol, 1 equiv) and diisopropylamine (87.0 μL, 64.6 mg, 500 μmol, 5 equiv) in dimethylformamide (2 mL). The solution was stirred for 1 h at 0 °C, and *tert*-butyl *N*-(3-aminopropyl)carbamate (57.5 mg, 330 μmol, 3.3 equiv) in dimethylformamide (500 μL) was added dropwise. The solution was stirred overnight at rt, quenched with water, and extracted with ethyl acetate (3 × 5 mL). The combined organic layers were washed with hydrochloric acid (1 M, 10 mL), saturated sodium hydrogen carbonate solution (10 mL), and saturated sodium chloride solution (3 × 10 mL). After removing the solvent and drying *in vacuo*, **15a** was obtained and used for the synthesis of **15** without further purification.

Compound ***15***. Trifluoroacetic acid (1 mL) was added to a solution of **15a** (100 μmol, 1 equiv) in dichloromethane (3 mL) at 0 °C over a time of 10 min with a syringe pump. The solution was stirred for 30 min at 0 °C and for 30 min at rt. After the addition of toluene (4 mL), the solvent was removed and the residue was dried *in vacuo*. The residue was dissolved in aqueous sodium hydrogen carbonate solution (0.5 M, 4 mL). Compound **6** (400 μmol, 4 equiv) in 1,4-dioxane (4 mL) was added to this solution at 0 °C over a time of 15 min. The reaction mixture was stirred at 0 °C for 5 min, warmed to rt, mixed with ice, and extracted with ethyl acetate (3 × 5 mL). The combined organic layers were washed with saturated solutions of sodium hydrogen carbonate and sodium chloride (2 × 10 mL each) and dried over sodium sulfate. After removing the solvent, **15** was obtained by purification *via* HPLC as a white solid (12.5 mg, 11.5 μmol, 12% over three steps).

^{1}H NMR (700 MHz, DMSO-d_6): δ [ppm] = 1.70−1.79 (m, 6H), 2.23 (s, 3H), 2.23 (s, 6H), 2.28 (s, 3H) 2.28 (s, 6H), 3.2−3.29 (m, 10H), 3.36 (dd, J = 13.0, 6.7 Hz, 2H) 7.34−7.39 (m, 6H), 7.43−7.47 (m, 3H), 8.16 (s, 2H), 8.37−8.41 (m, 3H), 8.87 (t, J = 5.6 Hz, 1H), 8.96 (t, J = 5.7 Hz, 2H).

^{13}C NMR (176 MHz, DMSO-d_6): δ [ppm] = 20.2, 20.2, 20.3, 28.8, 28.9, 36.8, 37.0, 37.2, 37.5, 125.3, 125.3, 125.9, 126.2, 126.3, 128.6, 131.1, 131.2, 131.4, 136.3, 139.9, 140.0, 132.8, 142.8, 147.9, 163.6, 163.9, 164.6, 167.8, 168.3.

$C_{51}H_{53}N_7O_{20}$ (1084.01), exact mass: 1083.3345.

ESI-HRMS (m/z): $[M + H]^+$ calcd for $C_{51}H_{54}N_7O_{20}$: 1084.3424; found: 1084.3418.

Compound ***16a***. 1,2,3-Trimethylbenzene (90%, 741 μL, 601 mg, 5.00 mmol, 1 equiv) was added to a solution of *N*-bromosuccinimide (3.54 g, 20.0 mmol, 4 equiv) in tetrachloromethane (15 mL). The reaction mixture was irradiated with a halogen lamp in a sealed glass vial, heated to 80 °C, and stirred overnight. The mixture was filtered and the filtrate was dried over sodium sulfate. After removing the solvent, **16a** was obtained by purification *via* automatic flash chromatography (PE/EA) but still obtained slight impurities. These were removed by washing the product with petrol ether and sonicating the mixture. After decanting and drying *in vacuo*, **16a** was obtained as a white solid (1.56 g, 4.38 mmol, 88%).

TLC R_f = 0.24 (PE).

^{1}H NMR (500 MHz, CD_2Cl_2): δ [ppm] = 4.65 (s, 4H), 4.84 (s, 2H), 7.46 (dd, J = 8.6, 6.6 Hz, 1H), 7.37−7.40 (m, 2H).

^{13}C NMR (125 MHz, CD_2Cl_2): δ [ppm] = 25.3, 30.5, 130.2, 132.3, 136.2, 138.7.

Compound ***16b***. Compound **16a** (2.18 g, 6.09 μmol) in dichloromethane (6 mL) was added to nitric acid (100%, 3.5 mL) in dichloromethane (2 mL) at −40 °C over a time of 2 h with a syringe pump. The temperature was kept strictly under −40 °C throughout the addition of the acid. The solution was stirred for 15 min at −40 °C and poured on ice. After the separation of the phases, the aqueous layer was extracted with dichloromethane (4 × 10 mL) and the combined organic layers were dried over sodium sulfate. After removing the solvent, **16b** (875 mg, 2.18 mmol, 36%) was obtained together with its nitration regioisomer by purification *via* automatic flash chromatography (PE/EA).

TLC R_f = 0.07 (PE).

^{1}H NMR (500 MHz, $CDCl_3$): δ [ppm] = 4.61 (s, 2H), 4.81 (s, 2H), 4.83 (s, 2H), 7.53 (d, J = 8.4 Hz,1 H), 7.85 (d, J = 8.4 Hz,1 H).

^{13}C NMR (125 MHz, $CDCl_3$): δ [ppm] = 22.4, 23.2, 28,0, 125.4, 131.9, 131.9, 132.2, 142.8, 149.7.

Compound ***16***. An aqueous solution of ammonia (30%, 1 mL) was added dropwise to a solution of **16b** (20.1 mg, 50 μmol, 1 equiv) in tetrahydrofuran and ethanol (500 μL each). The reaction mixture was stirred for 2.5 h. After removing the solvent and drying *in vacuo*, the residue was dissolved in aqueous sodium hydrogen carbonate solution (0.5 M, 2 mL). Compound **6** (200 μmol, 4 equiv) in 1,4-dioxane (2 mL) was added to this solution at 0 °C over a time of 15 min with a syringe pump. The reaction mixture was warmed to rt, mixed with ice, and extracted with ethyl acetate (3 × 5 mL). The combined organic layers were washed with a saturated solution of sodium chloride (2 × 100 mL) and dried over sodium sulfate. After removing the solvent, **16** was obtained by purification *via* HPLC as a white solid (12.8 mg, 14.7 μmol, 29% over 2 steps). It still contained *ca.* 10% of the respective nitration regioisomer.

^{1}H NMR (700 MHz, DMSO-d_6): δ [ppm] = 2.14 (s, 3H), 2.17 (s, 6H), 2.26 (s, 3H), 2.27 (s, 3H), 2.29 (s, 3H), 4.59 (d, J = 5.8 Hz, 2H), 4.70 (t J = 4.6 Hz, 4H), 7.28−7.43 (m, 8H), 7.50 (d, J = 8.5 Hz, 1H), 7.55 (dd, J = 7.2, 2.1 Hz, 1H), 7.86 (d, J = 8.5, Hz, 1H), 8.76 (t, J = 5.0 Hz, 1H), 8.78 (t, J = 4.9 Hz, 1H), 9.08 (t, J = 5.9 Hz, 1H).

^{13}C NMR (176 MHz, DMSO-d_6): δ [ppm] = 20.0, 20.0, 20.2, 20.3, 36.4, 36.5, 40.1, 123.2, 125.5, 125.6, 125.7, 125.9, 126.0, 126.1, 126.1, 126.1, 126.3, 127.2, 130.3, 130.6, 130.6, 131.0, 137.0, 140.0, 140.1, 142.8, 142.8, 143.8, 150.0, 164.4, 164.9, 167.7, 167.8, 167.9, 168.2, 168.2, 168.3.

$C_{42}H_{38}N_4O_{17}$ (870.78), exact mass: 870.2232.

ESI-HRMS (m/z): $[M + H]^+$ calcd for $C_{42}H_{39}N_4O_{17}$: 871.2310; found: 871.2303.

Compound ***17a***. Oxalyl chloride (690 μL, 1.02 g, 8.00 mmol, 4 equiv) was added to a solution of 5-Nitro-1,2,3-benzenetricarboxylic acid (510 mg, 2.00 mmol, 1 equiv) in dichloromethane (20 mL) and dimethylformamide (1 mL) at 0 °C over a time of 15 min with a syringe pump. The solution was stirred for 5 min at 0 °C and for 20 min at rt. After removing the solvent and drying *in vacuo*, the residue was taken up in dichloromethane (20 mL). *tert*-Butyl *N*-(2-aminoethyl)carbamate (1.04 mL, 1.06 g, 6.60 mmol, 3.3 equiv) and triethylamine (2.22 mL, 1.62 g, 16 mmol, 8 equiv) were added dropwise at 0 °C. The solution was stirred for 10 min at 0 °C and for 30 min at rt. After removing the solvent, the residue was taken up in ethyl acetate (25 mL). The organic layer was washed with saturated solutions of sodium hydrogen carbonate and sodium chloride (2 × 25 mL each). The combined organic layers were reextracted with ethyl acetate (2 × 25 mL) and dried over sodium sulfate. After removing the solvent and drying *in vacuo*, **17a** was obtained by purification *via*

https://doi.org/10.1021/acs.jmedchem.1c01482
J. Med. Chem. 2021, 64, 15440−15460

automatic flash chromatography (CH_2Cl_2/MeOH 30:1 → 20:1 → 10:1) as a light yellow solid (150 mg, 220 μmol, 11%).

TLC R_f = 0.22 (CH_2Cl_2/MeOH = 20:1).

^{1}H NMR (700 MHz, DMSO-d_6): δ [ppm] = 1.38 (s, 9H), 1.38 (s, 18 H),3.06−3.16 (m, 8H), 3.24 (dd, J = 11.5, 5.7 Hz, 4H), 6.53(t, J = 5.7 Hz, 1H), 6.87 (t, J = 5.9 Hz, 2H), 8.31 (t, J = 5.4 Hz, 1H), 8.41 (s, 2H), 8.65 (t, J = 5.4 Hz, 2H).

^{13}C NMR (176 MHz, DMSO-d_6): δ [ppm] = 28.2, 28.2, 38.9, 39.3, 39.8, 77.7, 77.7, 123.4, 137.4, 141.4, 146.1, 155.4, 155.7, 165.5, 165.7.

$C_{30}H_{47}N_7O_{11}$ (681.74), exact mass: 681.7440.

ESI-HRMS (m/z): $[M + H]^+$ calcd for $C_{30}H_{48}N_7O_{11}$: 682.3412; found: 682.3406.

Compound ***17***. Trifluoroacetic acid (3.5 mL) was added to a solution of **17a** (150 mg, 220 μmol, 1 equiv) in dichloromethane (10.5 mL) at 0 °C over a time of 15 min with a syringe pump. The solution was stirred for 30 min at 0 °C and for 15 min at rt. After the addition of toluene (11 mL), the solvent was removed and the residue was dried *in vacuo*. The residue was dissolved in aqueous sodium hydrogen carbonate solution (0.5 M, 20 mL). Compound **6** (770 μmol, 3.5 equiv) in 1,4-dioxane (20 mL) was added to this solution at 0 °C. The reaction mixture was stirred at 0 °C for 30 min, warmed to rt, mixed with ice, and extracted with ethyl acetate (3 × 25 mL). The combined organic layers were washed with saturated sodium chloride solution (2 × 50 mL) and dried over sodium sulfate. After removing the solvent, **17** was obtained by purification *via* HPLC as a white solid (124 mg, 119 μmol, 54% over two steps).

^{1}H NMR (500 MHz, DMSO-d_6): δ [ppm] = 2.21 (s, 6H), 2.23 (s, 3H), 2.28 (s, 9H), 3.23−3.29 (m, 2H), 3.29−3.39 (m, 10H), 7.30−7.39 (m, 6H), 7.53 (dd, J = 6.6, 2.8 Hz, 2H), 7.56 (dd, J = 7.4, 1.9 Hz, 1H), 8.18 (t, J = 5.7 Hz, 1H), 8.41−8.47 (m, 3H), 8.45 (s, 2H), 8.76 (t, J = 5.4 Hz, 2H).

^{13}C NMR (125 MHz, DMSO-d_6): δ [ppm] = 20.2, 20.2, 20.3, 38.6, 38.6, 38.7, 39.1, 123.6, 125.4, 126.0, 126.1, 130.7, 130.8, 137.2, 140.1, 140.2, 141.4, 142.8, 142.8, 146.2, 164.4, 164.8, 165.6, 165.9, 167.8, 168.3.

$C_{48}H_{47}N_7O_{20}$ (1041.93), exact mass: 1041.2876.

ESI-HRMS (m/z): $[M + H]^+$ calcd for $C_{48}H_{48}N_7O_{20}$: 1042.2954; found: 1042.2941.

Compound ***18a***. Oxalyl chloride (172 μL, 254 mg, 400 μmol, 5 equiv) was added to a solution of 5-nitro-1,2,3-benzenetricarboxylic acid (102 mg, 2.00 mmol, 1 equiv) in dichloromethane (7 mL) and dimethylformamide (150 μL) at 0 °C dropwise. The solution was stirred for 30 min at 0 °C and for 1 h at rt. After removing the solvent and drying *in vacuo*, the residue was taken up in dichloromethane (5 mL). To this solution, a solution of *tert*-butyl *N*-(3-aminopropyl)-carbamate (230 mg, 1.32 mmol, 3.3 equiv) and triethylamine (333 μL, 243 g, 2.4 mmol, 6 equiv) in dichloromethane (5 mL) was added dropwise at 0 °C over a time of 30 min. The solution was stirred for 1.5 h at 0 °C, quenched with ice, and washed with hydrochloric acid (1 M) and saturated sodium chloride solution (15 mL each). The combined organic layers were reextracted with dichloromethane (40 mL) and dried over sodium sulfate. After removing the solvent and drying *in vacuo*, **18a** was obtained by purification *via* automatic flash chromatography (CH_2Cl_2/MeOH 30:1 → 20:1 → 10:1) as a light yellow solid (97.0 mg, 134 μmol, 34%).

^{1}H NMR (500 MHz, DMSO-d_6): δ [ppm] = 1.38 (s, 27 H), 1.53 (dt, J = 14.2, 7.2 Hz,2 H), 1.57−1.63 (m, 4H), 2.95−3.02 (m, 6H), 3.10 (dd, J = 13.0, 6.6 Hz,2 H), 3.20 (dd,J = 12.9, 6.7 Hz,4 H), 6.70 (t, J = 5.7 Hz, 1H), 6.77 (t, J = 5.7 Hz, 2H), 8.13 (t, J = 5.5 Hz, 1H), 8.31 (s, 2H), 8.41 (t, J = 5.6 Hz, 2H).

^{13}C NMR (125 MHz, DMSO-d_6): δ [ppm] = 28.2, 28.8, 29.2, 36.7, 37.0, 37.4, 37.4, 77.4, 77.5, 123.1 137.5, 141.2, 146.1, 155.6, 165.3, 165.4.

Compound ***18***. Trifluoroacetic acid (2 mL) was added to a solution of **18a** (72.4 mg, 100 μmol, 1 equiv) in dichloromethane (6 mL) at 0 °C over a time of 15 min with a syringe pump. The solution was stirred for 30 min at 0 °C and for 30 min at rt. After the addition of toluene (8 mL), the solvent was removed and the residue was dried *in vacuo*. The residue was dissolved in aqueous sodium hydrogen carbonate solution (0.5 M, 10 mL). Compound **6** (350 μmol, 3.5 equiv) in 1,4-dioxane (6 mL) was added to this solution at 0 °C over a time of 20 min with a syringe pump. The reaction mixture was stirred at rt for 80 min, mixed with ice, and extracted with ethyl acetate (3 × 20 mL). The combined organic layers were washed with saturated sodium chloride solution (2 × 40 mL) and dried over sodium sulfate. After removing the solvent, **18** was obtained by purification *via* HPLC as a white solid (11.1 mg, 10.2 μmol, 10% over two steps).

^{1}H NMR (700 MHz, DMSO-d_6): δ [ppm] = 1.63−1.68 (m, 2H), 1.69−1.74 (m, 4H), 2.23 (s, 9H), 2.27 (s, 3H), 2.28 (s, 6H), 3.16−3.21 (m, 2H), 3.24−3.30 (m, 10H), 7.32−7.38 (m, 6H), 7.44−7.47 (m, 3H), 8.23 (t, J = 5.8 Hz, 1H), 8.28 (t, J = 5.8 Hz, 1H), 8.35 (s, 2H), 8.33−8.37 (m, 2H), 8.50 (t, J = 5.6 Hz, 2H).

^{13}C NMR (176 MHz, DMSO-d_6): δ [ppm] = 20.2, 20.3, 28.3, 28.7, 36.7, 36.7, 37.0, 123.2, 125.3, 125.9, 126.2, 126.2, 131.1, 131.2, 137.5, 139.4, 141.3, 142.8, 146.2, 164.5, 164.6, 165.3, 165.5, 167.8, 167.9, 168.3, 168.3.

$C_{51}H_{53}N_7O_{20}$ (1084.01), exact mass: 1083.3345.

ESI-HRMS (m/z): $[M + H]^+$ calcd for $C_{51}H_{54}N_7O_{20}$: 1084.3424; found: 1084.3408.

Compound ***19a***. EDCI (2.11 g, 11.0 mmol, 1.1 equiv) and HOBt (1.49 g, 11.0 mmol, 1.1 equiv) were added to a solution of 2,3-dimethoxybenzoic acid (1.82 g, 10.0 mmol, 1 equiv) and *N*,*N*-diisopropylethylamine (3.50 mL, 2.59 g, 20 mmol, 2 equiv) in dimethylformamide (20 mL) at 0 °C. The solution was stirred for 5 min at 0 °C and for 90 min at rt. *tert*-Butyl *N*-(3-aminopropyl)-carbamate (1.92 g, 11.0 mmol, 1.1 equiv) in dimethylformamide (5 mL) was added at 0 °C over a time of 10 min with a syringe pump. The solution was stirred overnight at rt, quenched with ice water, and extracted with ethyl acetate (3 × 30 mL). The combined organic layers were washed with hydrochloric acid (1 M) and saturated sodium chloride solution (2 × 75 mL each) and dried over sodium sulfate. After removing the solvent and drying *in vacuo*, **19a** was obtained and used for the synthesis of **19b** without further purification.

Compound ***19b***. Hydrogen chloride (4 M in 1,4-dioxane, 24 mL) was carefully added to **19a** at 0 °C. The solution was stirred for 2 h at rt. After removing the solvent, the residue was taken up in water, frozen in liquid nitrogen, and lyophilized. An aqueous solution of sodium hydroxide (2 M) was added until a pH value between 10 and 11 was reached. The resulting solution was again frozen in liquid nitrogen and lyophilized. The residue was taken up in acetone and ethyl acetate and sonicated. The precipitate was filtered off. After removing the solvent and drying *in vacuo*, **19b** was obtained as an amber-colored oil (1.98 g, 8.31 mmol, 83% over two steps)

^{1}H NMR (500 MHz, DMSO-d_6): δ [ppm] = 1.76−1.84 (m, 2H), 2.81−2.87 (m, 2H), 3.28−3.34 (m,2 H), 3.77 (s, 3H), 3.83 (s, 3H), 7.07−7.13 (m, 1H),7.12 (t, J = 9.0 Hz, 1H), 7.16 (dd, J = 7.7, 2.2 Hz, 1H), 7.83 (s_{br}, 2H), 8.36 (t, J = 5.9 Hz, 1H).

^{13}C NMR (125 MHz, DMSO-d_6): δ [ppm] = 27.4, 35.9, 36.7, 55.9, 60.9, 114.7, 120.4, 124.0, 130.1, 146.1, 152.5, 166.0.

$C_{12}H_{18}N_2O_3$ (238.29), exact mass: 238.1317.

ESI-HRMS (m/z): $[M + H]^+$ calcd for $C_{12}H_{19}N_2O_3$: 239.1396; found: 239.1391.

Compound ***19c***. EDCI (121 mg, 630 μmol, 3.5 equiv) was added to a solution of 2-nitrobenzene-1,3,5-tricarboxylic acid (45.9 mg, 180 μmol, 1 equiv) and *N*,*N*-diisopropylethylamine (377 μL, 279 mg, 2.16 mmol, 12 equiv) in dimethylformamide (2 mL) at 0 °C. The solution was stirred for 5 min at 0 °C, and HOBt (85.1 mg, 630 μmol, 3.5 equiv) was added. The solution was stirred for 90 min at rt and the hydrochloride of **19b** (198 mg, 720 μmol, 4 equiv) in dimethylformamide (2 mL) was added at 0 °C over a time of 10 min with a syringe pump. The solution was stirred overnight at rt. 1,4-Dioxane was added, and the solution was frozen in liquid nitrogen and lyophilized. Compound **19c** was obtained by purification *via* HPLC as a white solid (42.5 mg, 46.6 μmol, 26%)

^{1}H NMR (500 MHz, methanol-d_4): δ [ppm] = 1.85−2.94 (m, 6H), 3.43−3.49 (m, 6H), 3.49−3.54 (m, 6H), 3.87 (s, 9H), 3.88 (s, 3H), 3.89 (s, 6H), 7.09−7.16 (m, 6H), 7.31 (dd, J = 7.4, 2.0 Hz, 1H),

https://doi.org/10.1021/acs.jmedchem.1c01482
J. Med. Chem. 2021, 64, 15440−15460

7.34(dd, J = 7.4, 2.1 Hz, 2H), 8.20 (s, 2H), 8.59 (t, J = 5.9 Hz, 1H),8.62 (t, J = 6.0 Hz, 2H).

^{13}C NMR (125 MHz, methanol-d_4): δ [ppm] = 30.4, 30.5,38.0, 38.2, 38.5, 38.8, 56.7, 62.1, 116.7, 116.8, 122.5, 122.6, 125.5, 125.5,129.3, 129.4, 130.2, 133.3, 138.5, 148.8, 148.9, 149.8, 154.4, 166.7, 167.2, 168.8, 168.9.

$C_{45}H_{53}N_7O_{14}$ (915.95), exact mass: 915.3650.

ESI-HRMS (m/z): $[M + Na]^+$ calcd for $C_{45}H_{53}N_7NaO_{14}$: 938.3548; found: 938.3540.

Compound ***19***. Boron tribromide (1 M in dichloromethane, 436 μL, 436 μmol, 18 equiv) was added dropwise to a solution of **19c** (22.2 mg, 24.2 μmol, 1 equiv) in dichloromethane (5 mL) at −78 °C. The reaction mixture was stirred at −78 °C for 1 h, slowly warmed to rt, quenched with ice water and methanol, and extracted with ethyl acetate (3 × 15 mL). The combined organic layers were dried over sodium sulfate. After removing the solvent, **19** was obtained by purification *via* HPLC as a brownish solid (10.4 mg, 12.5 μmol, 52%).

^{1}H NMR (500 MHz, DMSO-d_6): δ [ppm] = 1.73−1.87 (m, 6H), 3.28 (dd, J = 12.5, 6.3 Hz, 4H), 3.32−3.42 (m,8 H) 6.68 (t, J = 7.9 Hz, 3H), 6.91 (d, J = 7.6 Hz, 3H), 7.27 (d, J = 8.0 Hz, 3H), 8.16 (s, 2H), 8.76−8.83 (m, 3H), 8.89 (t, J = 5.2 Hz, 1H), 8.98 (t, J = 5.4 Hz, 2H), 9.14 (s_{br}, 3H), 12.72 (s_{br}, 3H).

^{13}C NMR (125 MHz, DMSO-d_6): δ [ppm] = 28.7, 28.9, 36.8, 36.9, 37.3, 37.5, 115.0, 115.0, 117.1, 117.9, 118.8, 128.7, 131.4, 136.3, 146.2, 147.9, 149.6, 149.7, 163.7, 163.9, 169.8, 169.6.

$C_{39}H_{41}N_7O_{14}$ (831.69), exact mass: 831.2711.

ESI-HRMS (m/z): $[M + H]^+$ calcd for $C_{39}H_{42}N_7O_{14}$: 832.2790; found: 832.2783.

Compound ***20a***. EDCI (121 mg, 630 μmol, 3.5 equiv) was added to a solution of 1,3,5-tricarboxylic acid (37.8 mg, 180 μmol, 1 equiv) and *N*,*N*-diisopropylethylamine (377 μL, 279 mg, 2.16 mmol, 12 equiv) in dimethylformamide (3 mL) at 0 °C. The solution was stirred for 5 min at 0 °C, and HOBt (85.1 mg, 630 μmol, 3.5 equiv) was added. The solution was stirred for 2.5 h at rt and the hydrochloride of **19b** (198 mg, 720 μmol, 4 equiv) in dimethylformamide (2 mL) was added at 0 °C over a time of 10 min with a syringe pump. The solution was stirred overnight, quenched with ice and hydrochloric acid (1 M), and extracted with ethyl acetate (5 × 10 mL). The precipitate from the organic layers was collected and dissolved in acetone. The combined organic layers were dried over sodium sulfate. After removing the solvent, **20a** was obtained by purification *via* flash chromatography (CH_2Cl_2/MeOH 20:1 → 15:1 → 10:1) as a white solid (38.2 mg, 43.9 μmol, 24%).

TLC R_f = 0.20 (CH_2Cl_2/MeOH = 20:1).

^{1}H NMR (500 MHz, methanol-d_4): δ [ppm] = 1.91 (p, J = 6.6 Hz, 6H), 3.51 (td, J = 13.3, 6.6 Hz, 12 H), 3.86 (s, 9H), 3.88 (s, 9H), 7.08−7.15 (m, 6H), 7.32 (dd, J = 7.4, 2.1 Hz, 3H), 8.43 (s, 3H).

^{13}C NMR (125 MHz, methanol-d_4): δ [ppm] = 30.6, 38.3, 38.7, 56.7, 62.1, 116.7, 122.5, 125.5, 129.4, 130.0, 136.8, 148.8, 154.4, 168.8, 168.9.

$C_{45}H_{54}N_6O_{12}$ (870.96), exact mass: 870.3800.

ESI-HRMS (m/z): $[M + Na]^+$ calcd for $C_{45}H_{54}N_6NaO_{12}$: 893.3697; found: 893.3690.

Compound ***20***. Boron tribromide (1 M in dichloromethane, 3.75 mL, 3.75 mmol, 18 equiv) was added dropwise to a solution of **20a** (181 mg, 208 μmol, 1 equiv) in dichloromethane (10 mL) at −78 °C. The reaction mixture was stirred at −78 °C for 1 h, slowly warmed to rt overnight. Since conversion was not complete, another batch of boron tribromide (1 M in dichloromethane, 1.25 mL, 1.25 mmol, 6 equiv) was added at −78 °C. The reaction mixture was stirred at −78 °C for 1 h, slowly warmed to rt overnight, quenched with ice water and methanol, and extracted with ethyl acetate (25 mL). The precipitate from the organic layers was collected and dissolved in methanol. The combined organic layers were dried over sodium sulfate. After removing the solvent, **20** was obtained by purification *via* HPLC as a brownish solid (67.5 mg, 85.8 μmol, 41%).

^{1}H NMR (500 MHz, DMSO-d_6): δ [ppm] = 1.83 (p, J = 7.0 Hz, 6H), 3.32−3.40 (m,12 H) 6.68 (t, J = 8.0 Hz, 3H), 6.90 (dd, J = 7.8, 1.4 Hz, 3H), 7.27 (dd, J = 8.2, 1.4 Hz, 3H), 8.42 (s, 3H), 8.76 (t, J = 5.7 Hz, 3H), 8.81 (t, J = 5.7 Hz, 3H), 9.11 (s_{br}, 3H), 12.75 (s_{br}, 3H).

^{13}C NMR (125 MHz, DMSO-d_6): δ [ppm] = 29.0, 36.9, 37.3, 115.0, 117.0, 117.9, 118.8, 128.4, 135.0, 146.2, 149.6, 165.6, 169.7.

$C_{39}H_{42}N_6O_{12}$ (786.80), exact mass: 786.2861.

ESI-HRMS (m/z): $[M + H]^+$ calcd for $C_{39}H_{43}N_6O_{12}$: 787.2939; found: 787.2934.

Compound ***21***. Zinc dust (574 mg, 7.79 mmol, 15 equiv) was added to a solution of **8** (510 mg, 586 μmol, 1 equiv) in tetrahydrofuran (4 mL), ethanol (3.2 mL), and acetic acid (800 μL) at 0 °C. The reaction mixture was stirred for 10 min at 0 °C and for 20 min at rt. It was filtered over celite and the precipitate was washed with ethyl acetate. The organic layer was washed with saturated solutions of sodium hydrogen carbonate and sodium chloride (2 × 30 mL each) and dried over sodium sulfate. After removing the solvent, crude product **21** was dried *in vacuo* and used in subsequent reactions without further purification.

Compound ***22***. *N*-methylmorpholine (257 μL, 237 mg, 2.34 mmol, 4 equiv) and isobutyl chloroformate (224 μL, 240 mg, 1.76 mmol, 3 equiv) were added to a solution of 5-hexynoic acid (226 μL, 230 mg, 2.05 mmol, 3.5 equiv) in tetrahydrofuran (6 mL) dropwise at 0 °C, whereupon a white precipitate formed immediately. The reaction mixture was stirred for 10 min at 0 °C and for 90 min at rt. Compound **21** (586 μmol, 1 equiv) in tetrahydrofuran (5 mL) was added at 0 °C over a time of 10 min with a syringe pump at 0 °C. The reaction mixture was stirred overnight at rt, quenched with ice and saturated sodium hydrogen carbonate solution (*ca.* 5 mL each), and extracted with ethyl acetate (3 × 10 mL). The organic layer was washed with hydrochloric acid (0.1 M) and saturated solutions of sodium hydrogen carbonate and sodium chloride (2 × 25 mL each) and dried over sodium sulfate. After removing the solvent, **22** was obtained by purification *via* automatic flash chromatography (CH_2Cl_2/MeOH) as a white solid (233 mg, 249 μmol, 43%).

TLC R_f = 0.19 (CH_2Cl_2/MeOH = 20:1).

^{1}H NMR (700 MHz, DMSO-d_6): δ [ppm] = 1.80 (p, J = 7.2 Hz,2 H), 2.16 (s, 3H), 2.17 (s, 6H), 2.25 (td, J = 7.1, 2.6 Hz, 2H), 2.28 (s, 3H), 2.28 (s, 6H), 2.51 (t,J = 7.5 Hz, 2H), 2.81 (t, J = 2.6 Hz,1 H), 4.33 (s_{br}, 4H) 4.38(d, J = 5.9 Hz, 2H), 7.21 (s, 2H), 7.23 (t, J = 7.9 Hz, 1H), 7.31 (t, J = 7.9 Hz, 2H), 7.35 (dd, J = 8.1, 1.5 Hz, 1H), 7.38 (dd, J = 8.1, 1.5 Hz, 2H), 7.44 (dd, J = 7.8, 1.5 Hz, 1H), 7.53 (dd, J = 7.7, 1.5 Hz, 2H), 8.78 (t, J = 6.0 Hz, 2H), 8.94 (t, J = 6.0 Hz, 1H), 9.54 (s, 1H).

^{13}C NMR (176 MHz, DMSO-d_6): δ [ppm] = 17.5, 20.2, 20.3, 24.1, 34.1, 39.1, 42.2, 71.6, 84.0, 124.6, 125.4, 125.5, 126.0, 126.1, 126.2, 130.6, 130.6, 131.8, 153.8, 137.5, 140.1, 132.8, 164.5, 164.7, 167.8, 167.9, 168.3, 171.1.

$C_{48}H_{46}N_4O_{16}$ (934.91), exact mass: 934.2909.

ESI-HRMS (m/z): $[M + H]^+$ calcd for $C_{48}H_{47}N_4O_{16}$: 935.2987; found: 935.2985.

Compound ***23***. Triethylamine (1 mL) was added to a solution of **22** (80 mg, 85.6 μmol) in methanol (3 mL) dropwise at 0 °C. This solution was stirred for 5 min at 0 °C and for 2.5 h at rt, quenched with ice, acidified with hydrochloric acid (2 M), and extracted with ethyl acetate (3 × 3 mL). The combined organic layers were dried over sodium sulfate. After removing the solvent, **23** was obtained by purification *via* HPLC as a white solid (39.5 mg, 57.9 μmol, 68%).

^{1}H NMR (700 MHz, DMSO-d_6): δ [ppm] = 1.79 (p, J = 7.2 Hz,2 H), 2.24 (td, J = 7.1, 2.6 Hz, 2H), 2.49−2.53 (m, 2H), 2.81 (t, J = 2.6 Hz,1 H), 4.40 (d, J = 5.9 Hz, 2H), 4.43 (s_{br}, 4H) 6.60 (t, J = 7.9 Hz, 1H), 6.67 (t,J = 7.9 Hz, 2H), 6.88 (dd, J = 7.8, 1.3 Hz, 1H), 6.92 (dd, J = 7.8, 1.3 Hz, 2H), 7.19−7.21 (m, 1H), 7.20 (s, 2H), 7.29 (dd, J = 8.2, 1.3 Hz, 2H), 9.15 (s_{br}, 3H), 9.15 (t, J = 6.0 Hz, 2H), 9.32 (t, J = 7.2 Hz, 1H), 9.57 (s, 1H), 12.52 (s_{br}, 2H), 12.57 (s_{br}, 1H).

^{13}C NMR (176 MHz, DMSO-d_6): δ [ppm] = 17.5, 24.1, 34.1, 39.0, 42.1, 71.6, 84.0, 114.9, 115.1, 117.1, 117.3, 117.9, 118.0, 118.8, 118.9, 124.8, 132.1, 135.9, 137.4, 146.1, 146.2,149.5, 149.6, 169.7, 169.8, 171.2.

$C_{36}H_{34}N_4O_{10}$ (682.69), exact mass: 682.2275.

ESI-HRMS (m/z): $[M + Na]^+$ calcd for $C_{36}H_{34}N_4NaO_{10}$: 705.2173; found: 705.2170.

Compound ***24a***. Lithium-bis(trimethylsilyl)amide (1 M in tetrahydrofuran, 22 mL, 22 mmol, 1.1 equiv) was added to a solution

https://doi.org/10.1021/acs.jmedchem.1c01482
J. Med. Chem. 2021, 64, 15440−15460

of methyl-2-phenyl acetate (2.82 mL, 3.00 g, 20.0 mmol, 1 equiv) in tetrahydrofuran (50 mL) over a time of 20 min with a syringe pump at −50 °C. The reaction mixture was stirred for 1 h at −50 °C, warmed to −20 °C, and 6-iodo-1-hexyne (2.90 mL, 4.58 g, 22.0 mmol, 1.1 equiv) in tetrahydrofuran (5 mL) was added over a time of 20 min with a syringe pump. The reaction mixture was warmed to 0 °C, stirred for 1 h, quenched with ice, and mixed with saturated ammonium chloride solution (50 mL). After separation of the phases, the aqueous layer was extracted with diethyl ether (2 × 50 mL), and the combined organic layers were dried over sodium sulfate. After removing the solvent crude product, **24a** was dried *in vacuo* and for the synthesis of **24b** without further purification.

*Compound **24b***. Potassium hydroxide (1.68 g, 30.0 mmol, 1.5 equiv) was added to a solution of **24a** (20.0 mmol, 1 equiv) in methanol (100 mL) and water (2 mL). The reaction mixture was refluxed overnight and cooled to room temperature. After removing the solvent, the crude product was taken up in water (30 mL) and washed with diethyl ether. The aqueous layer was acidified with hydrochloric acid (6 M) to pH ≈ 1 and extracted with diethyl ether (3 × 30 mL). The combined organic layers were dried over sodium sulfate. After removing the solvent, **24b** was obtained by purification *via* flash chromatography (CH_2Cl_2/MeOH 100:0 → 99:1 → 97:3, 1% AcOH) as a white solid (3.08 g, 14.2 mmol, 71%).

TLC R_f = 0.29 (CH_2Cl_2/MeOH = 80:3, 1% AcOH).

^{1}H NMR (500 MHz, DMSO-d_6): δ [ppm] = 1.19−1.27 (m, 1H), 1.27−1.36 (m, 1H), 1.39−1.49 (m, 2H), 1.60−1.69 (m, 1H), 1.90−1.99 (m, 1H), 2.11 (td, J = 7.0, 2.6 Hz, 2H), 2.70 (t, 2.6 Hz, 1H), 3.48 (t, J = 7.6 Hz, 1H), 7.22−7.26 (m, 1H), 7.27−7.34 (m, 4H), 12.3 (s, 1H).

^{13}C NMR (125 MHz, DMSO-d_6): δ [ppm] = 17.6, 26.3, 27.7, 32.5, 50.8, 71.2, 84.3, 126.8, 127.7, 128.4, 139.7, 174.8.

$C_{14}H_{16}O_2$ (216.28).

*Compound **24c***. Oxalyl chloride (1.72 mL, 2.54 g, 20.0 mmol, 2 equiv) was added to a solution of **22b** (2.16 g, 10.0 mmol, 1 equiv) in dichloromethane (10 mL) over a time of 10 min with a syringe pump. After the addition of one drop of dimethylformamide the solution was stirred for 1 h. The solvent was removed while stirring *in vacuo* under stirring using a cooling trap. The residue was taken up in tetrahydrofuran (20 mL) and triethylamine (5.50 mL, 4.05 g, 40.0 mmol, 4 equiv) was added at 0 °C. The solution was stirred for 2 h at 0 °C, and the resulting precipitate was filtered off over a Schlenk-frit. The solvent was distilled off at 110 °C, and the residue was purified *via* distillation at 3 mbar at a temperature of 110 °C increasing to 150 °C. Compound **24c** was isolated from the main run as a yellow oil (433 mg, 2.18 mmol, 22%). Since Ketene **24c** was unstable under atmospheric conditions, all work steps were conducted under Schlenk conditions.

^{1}H NMR (500 MHz, $CDCl_3$): δ [ppm] = 1.54−1.67 (m, 4H), 1.88 (t, J = 2.7 Hz, 1H), 2.16 (td, J = 6.8, 2.6 Hz, 2H), 2.34−2.38 (m, 2H), 6.94−7.02 (m, 3H), 7.21−7.25 (m, 2H),

^{13}C NMR (125 MHz, $CDCl_3$): δ [ppm] = 18.2, 23.2, 27.1, 28.0, 39.2, 68.7, 84.0, 124.1, 124.3, 129.0, 132.5, 204.6.

$C_{14}H_{14}O$ (198.27).

*Compound **24***. Compound **24c** (65.4 mg, 330 μmol, 1.2 equiv) in tetrahydrofuran (800 μL) was added to a solution of **21** (231 mg, 275 μmol, 1 equiv) in tetrahydrofuran (2 mL) at 0 °C. The solution was stirred for 10 min at 0 °C and overnight at rt. Another batch of **24c** (32.7 mg, 165 μmol, 0.6 equiv) was added and the solution was stirred overnight. After removing the solvent, the crude product was purified *via* flash chromatography (CH_2Cl_2/MeOH 80:2 → 80:3). Since the purity of the target compound was not adequate, **24** was obtained by further purification *via* HPLC as a white solid (80.0 mg, 77.0 μmol, 28%).

TLC R_f = 0.29 (CH_2Cl_2/MeOH = 80:3).

^{1}H NMR (700 MHz, DMSO-d_6): δ [ppm] = 1.34−1.40 (m, 1H), 1.41−1.47 (m, 1H),

1.47−1.57 (m, 2H), 1.69−1.75 (m, 1H), 2.08−2.14 (m, 1H), 2.14 (s, 3H), 2.14−2.17 (m, 2H), 2.16 (s, 6H), 2.27 (s, 3H), 2.29 (s, 6H), 2.68 (t, J = 2.6 Hz, 1H), 3.80 (dd, J = 8.6, 6.6 Hz, 1H), 4.18 (s_{br}, 4H), 4.36 (d, J = 5.9 Hz, 2H), 7.15 (s, 2H), 7.20 (t, J = 7.9 Hz, 1H), 7.22−7.26 (m, 1H), 7.28−7.35 (m, 5H), 7.38 (dd, J = 8.1, 1.4 Hz, 2H), 7.41 (dd, 7.8, 1.5 Hz, 1H), 7.44 (d, J = 7.2 Hz, 2H), 7.50 (d, J = 6.1 Hz, 2H), 8.70 (s_{br}, 2H), 8.93 (t, J = 6.0 Hz, 1H), 9.79 (s, 1H).

^{13}C NMR (176 MHz, DMSO-d_6): δ [ppm] = 17.6, 20.1, 20.3, 26.5, 27.8, 32.1, 38.8, 42.2, 51.4, 71.1, 84.4, 124.0, 125.4, 125.6, 126.0, 126.0, 126.2, 126.8, 127.6, 128.4, 130.5, 130.6, 131.2, 135.8, 137.7, 140.1, 140.1, 140.6, 142.8, 142.8.

$C_{56}H_{54}N_4O_{16}$ (1039.06), exact mass: 1038.3535.

ESI-HRMS (m/z): $[M + H]^+$ calcd for $C_{56}H_{55}N_4O_{16}$: 1039.3613 found: 1039.3605.

*Compound **25a***. Sodium azide (3.25 g, 50 mmol, 5 equiv) was added to a solution of 3-bromoproionic acid (1.53 g, 10 mmol, 1 equiv) in water (20 mL). The solution was stirred for 4 h at rt, carefully acidified with hydrochloric acid to pH ≈ 1, and extracted with ethyl acetate (3 × 30 mL). The combined organic layers were washed with saturated sodium chloride solution (50 mL) and dried over sodium sulfate. After removing the solvent, **25a** was obtained as a pale yellow oil (1.04 g, 9.00 mmol, 90%).

*Compound **25***. *N*-methylmorpholine (5.50 μL, 5.06 mg, 50 μmol, 1 equiv) and isobutyl chloroformate (6.36 μL, 6.83 mg, 50 μmol, 1 equiv) were added to a solution of **25a** (7.75 mg, 50 μmol, 1 equiv) in tetrahydrofuran (2 mL) at 0 °C, whereupon a white precipitate formed immediately. The reaction mixture was stirred for 2 h at 0 °C. A solution of ampicillin (11.2 mg, 55 μmol, 1.1 equiv) and triethylamine (20.0 μL, 14.5 mg, 144 μmol, 2.87 equiv) in tetrahydrofuran (1 mL) and water (200 μL) was added at 0 °C. The reaction mixture was stirred for 1 h at 0 °C and for 1 h at rt. After removing the solvent, the residue was taken up in water (*ca.* 4 mL) and acidified with hydrochloric acid (1 M) to pH ≈ 2. The resulting suspension was extracted with ethyl acetate (3 × 5 mL) and the combined organic layers were washed with saturated sodium chloride solution (15 mL) and dried over sodium sulfate. After removing the solvent, **25** was obtained by purification *via* HPLC as a white solid (13.3 mg, 29.8 μmol, 60%).

^{1}H NMR (500 MHz, DMSO-d_6): δ [ppm] = 1.41 (s, 3H), 1.56 (s, 3H), 2.54 (td, J = 6.3, 2.3, 2H), 3.46−3.55 (m, 2H), 4.21 (s, 1H), 5.40 (d, J = 4.0 Hz, 1H), 5.52 (dd, J = 7.8, 4.0 Hz, 1H), 5.77 (d, J = 8.2 Hz, 1H), 7.24−7.29 (m, 1H), 7.30−7.35 (m, 2H), 7.43 (d, J = 7.3 Hz, 2H), 8.73 (d, J = 8.2 Hz, 1H), 9.16 (d, J = 7.9 Hz, 1H), 13.32 (s_{br}, 1H).

^{13}C NMR (125 MHz, DMSO-d_6): δ [ppm] = 26.6, 30.4, 34.2, 46.9, 55.4, 58.1, 63.7, 67.2, 70.3, 127.1, 127.5, 128.2, 138.1, 168.9, 169.3, 170.0, 173.4.

$C_{19}H_{22}N_6O_5S$ (446.48), exact mass: 446.1372.

ESI-HRMS (m/z): $[M + H]^+$ calcd for $C_{19}H_{23}N_6O_5S$: 447.1451; found: 447.1445.

*Compound **26***. *N*-Methylmorpholine (165 μL, 152 mg, 1.50 μmol, 1 equiv) and isobutyl chloroformate (191 μL, 205 mg, 150 mmol, 1 equiv) were added to a solution of **25a** (233 mg, 1.50 mmol, 1 equiv) in tetrahydrofuran (10 mL) at 0 °C, whereupon a white precipitate formed immediately. The reaction mixture was stirred for 30 min at 0 °C and for 30 min at rt. A solution of amoxicillin (603 mg, 1.65 mmol, 1.1 equiv) and triethylamine (627 μL, 455 mg, 4.50 mmol, 3 equiv) in tetrahydrofuran (5 mL) and water (1 mL) was added at 0 °C. The reaction mixture was stirred for 30 min at 0 °C and for 30 min at rt. After removing the solvent, the residue was taken up in ice water and acidified with hydrochloric acid (1 M) to pH ≈ 2. The resulting suspension was extracted with ethyl acetate (3 × 10 mL) and the combined organic layers were washed with saturated sodium chloride solution (30 mL) and dried over sodium sulfate. After removing the solvent, **26** was obtained by purification *via* automatic flash chromatography over a reversed-phase column as a white solid (123 mg, 266 μmol, 18%).

^{1}H NMR (500 MHz, DMSO-d_6): δ [ppm] = 1.42 (s, 3H), 1.56 (s, 3H), 2.45−2.55 (m, 2H), 3.45−3.54 (m, 2H), 4.21 (s, 1H), 5.39 (d, J = 4.1 Hz, 1H), 5.52 (dd, J = 8.0, 4.1 Hz, 1H), 5.60 (d, J = 8.1 Hz, 1H), 6.66−6.71 (m, 2H), 7.17−7.23 (m, 2H), 8.57 (d, J = 8.1 Hz, 1H), 8.98 (d, J = 8.0 Hz, 1H), 9.37 (s_{br}, 1H), 13.33 (s_{br}, 1H).

https://doi.org/10.1021/acs.jmedchem.1c01482
J. Med. Chem. 2021, 64, 15440−15460

^{13}C NMR (125 MHz, DMSO-d_6): δ [ppm] = 26.6, 30.3, 34.2, 46.9, 54.9, 80.0, 63.7, 67.2, 70.3, 114.9, 128.3, 128.3, 156.8, 168.9, 169.1, 170.5, 173.6.

$C_{19}H_{22}N_6O_6S$ (462.48), exact mass: 462.1322.

ESI-HRMS (m/z): [M + H]$^+$ calcd for $C_{19}H_{23}N_6O_6S$: 463.1400; found: 463.1395.

Compound ***27***. TBTA (2.65 mg, 5.00 μmol, 0.5 equiv) in dimethylformamide (50 μL) was added to a solution of **22** (18.7 mg, 20.0 μmol, 2 equiv) and **25** (4.46 mg, 10.0 μmol, 1 equiv) in dimethylformamide (400 μL) and PBS buffer (100 μL). A mixture of copper(II) sulfate (400 μg, 2.50 μmol, 0.25 equiv) and sodium ascorbate (990 μg, 5.00 μmol, 0.5 equiv) in water (100 μL) was added. This step was repeated after stirring for 45 min at rt and the solution was again stirred for 45 min at rt. Another batch of TBTA (2.65 mg, 5.00 μmol, 0.5 equiv) in dimethylformamide (50 μL) was added to the solution. An identical amount of the mixture consisting of copper(II) sulfate and sodium ascorbate in water (*v.s.*) was added. This step was repeated after stirring for 45 min at rt. After another 45 min of stirring at rt **27** was obtained by purification of the solution *via* HPLC as a white solid (11.0 mg, 7.96 μmol, 80%).

^{1}H NMR (700 MHz, DMSO-d_6): δ [ppm] = 1.40 (s, 3H), 1.54 (s, 3H), 1.89−1.95 (m, 2H), 2.15 (s, 6H), 2.16 (s, 3H), 2.28 (s, 3H), 2.28 (s, 6H), 2.46 (t, J = 7.5 Hz, 2H), 2.67 (t, J = 7.6 Hz, 2H), 2.79−2.85 (m, 1H), 2.86−2.92 (m, 1H), 4.17 (s, 1H), 4.34 (s_{br}, 4H), 4.38 (d, J = 5.8, Hz, 2H), 4.51 (td, J = 13.7, 7.0 Hz, 2H), 5.38 (d, J = 3.9 Hz, 1H), 5.50 (dd, J = 7.8, 4.0 Hz, 1H), 5.73 (d, J = 8.1 Hz, 1H),7.21 (s, 2H), 7.23 (t,J = 7.9 Hz, 1H), 7.26 (t,J = 7.2 Hz, 1H), 7.30(t, J = 7.9 Hz, 4H), 7.33−7.39 (m, 5H), 7.44 (dd, J = 7.7, 1.4 Hz, 1H), 7.52 (dd, J = 7.7, 1.4 Hz, 2H), 7.76 (s, 1H), 8.73 (d, J = 8.1 Hz, 1H), 8.78(t, J = 6.0 Hz, 2H), 8.94(t, J = 6.0 Hz, 1H), 9.16 (d, J = 7.8 Hz, 1H), 9.51 (s, 1H),13.30 (s_{br}, 1H).

^{13}C NMR (176 MHz, DMSO-d_6): δ [ppm] = 20.1, 20.2, 20.3, 24.8, 25.1, 26.7, 30.4, 34.9, 35.2, 39.1, 42.2, 45.6, 55.4, 58.0, 63.8, 67.1, 69.8, 121.9, 124.6, 125.4, 125.5, 126.0, 126.0, 126.1, 126.2, 127.0. 127.5, 128.2, 130.6, 130.7, 131.8, 135.8, 137.5, 138.0, 140.1, 140.1, 142.8, 146.2, 164.5, 164.7, 167.8, 167.9, 168.3, 168.9, 168.9, 169.9, 171.5, 173.3.

$C_{67}H_{68}N_{10}O_{21}S$ (1381.39), exact mass: 1380.4281.

ESI-HRMS (m/z): [M + H]$^+$ calcd for $C_{67}H_{69}N_{10}O_{21}S$: 1381.4359; found: 1381.4366.

Compound ***28***. TBTA (2.65 mg, 5.00 μmol, 0.5 equiv) in dimethylformamide (50 μL) was added to a solution of **23** (13.7 mg, 20.0 μmol, 2 equiv) and **25** (4.46 mg, 10.0 μmol, 1 equiv) in dimethylformamide (400 μL) and PBS buffer (100 μL). A mixture of copper(II) sulfate (400 μg, 2.50 μmol, 0.25 equiv) and sodium ascorbate (990 μg, 5.00 μmol, 0.5 equiv) in water (100 μL) was added. This step was repeated after stirring for 45 min at rt and the solution was again stirred for 45 min at rt. Another batch of TBTA (2.65 mg, 5.00 μmol, 0.5 equiv) in dimethylformamide (50 μL) was added to the solution. An identical amount of the mixture consisting of copper(II) sulfate and sodium ascorbate in water (*v.s.*) was added. This step was repeated after stirring for 45 min at rt. After another 45 min of stirring at rt **28** was obtained by purification of the solution *via* HPLC as a white solid (4.50 mg, 3.98 μmol, 40%).

^{1}H NMR (700 MHz, DMSO-d_6): δ [ppm] = 1.40 (s, 3H), 1.54 (s, 3H), 1.88−1.94 (m, 2H), 2.46 (t, J = 7.5 Hz, 2H), 2.66 (t, J = 7.6 Hz, 2H), 2.79−2.84 (m, 1H), 2.86−2.92 (m, 1H), 4.19 (s, 1H), 4.40 (d, J = 5.8, Hz, 2H), 4.44 (s_{br}, 4H), 4.47−4.55 (m, 2H), 5.39 (d, J = 4.0 Hz, 1H), 5.51 (dd, J = 7.9, 4.0 Hz, 1H), 5.73 (d, J = 8.1 Hz, 1H), 6.60 (t, J = 7.9 Hz,1 H),6.67 (t, J = 7.9 Hz,2 H), 6.88 (dd, J = 7.8, 1.3 Hz, 1H), 6.92 (dd, J = 7.8, 1.2 Hz, 2H), 7.18−7.21 (m, 1H), 7.20 (s, 2H), 7.23−7.27 (m, 1H), 7.27−7.31 (m, 4H), 7.33−7.36 (m, 2H), 7.75 (s, 1H), 8.72 (d, J = 8.1 Hz, 1H), 9.08 (s_{br}, 1H), 9.13−9.18 (m, 5H), 9.32 (t, J = 6.0 Hz, 1H), 9.54 (s, 1H), 12.52 (s, 2H), 12.57 (s, 1H), 13.32 (s_{br}, 1H).

^{13}C NMR (176 MHz, DMSO-d_6): δ [ppm] = 24.8, 25.1, 26.6, 30.3, 34.8, 35.2, 38.9, 42.1, 45.6, 55.4, 58.1, 63.7, 67.2, 70.3, 114.9, 115.1, 117.1, 117.3, 117.9, 118.0, 118.8, 118.9, 121.9, 124.8, 127.0, 127.5, 128.1, 132.1, 135.9, 137.4, 138.0, 146.1, 146.2, 146.2, 149.5, 149.6, 168.9, 168.9, 169.7, 169.8, 169.9, 171.5, 173.3.

$C_{55}H_{56}N_{10}O_{15}S$ (1129.17), exact mass: 1128.3647.

ESI-HRMS (m/z): [M + H]$^+$ calcd for $C_{55}H_{57}N_{10}O_{15}S$: 1129.3726; found: 1129.3713.

Compound ***29***. A mixture of copper(II) sulfate (800 μg, 5.00 μmol, 0.25 equiv) and sodium ascorbate (1.98 mg, 10.0 μmol, 0.5 equiv) in water (100 μL) was added to a solution of **22** (28.0 mg, 30.0 μmol, 1.5 equiv) and **26** (9.25 mg, 20.0 μmol, 1 equiv) in dimethylformamide (500 μL). The solution was stirred for 30 min at rt. The addition of an equal mixture of copper(II) sulfate and sodium ascorbate in water was repeated three times. After each addition, the solution was stirred for 30 min. Compound **29** was obtained by purification of the solution *via* HPLC as a white solid (10.5 mg, 7.51 μmol, 38%).

^{1}H NMR (700 MHz, DMSO-d_6): δ [ppm] = 1.42 (s, 3H), 1.56 (s, 3H), 1.91−1.97 (m, 2H), 2.16 (s, 6H), 2.17 (s, 3H), 2.29 (s, 3H), 2.29 (s, 6H), 2.47 (t, J = 7.5 Hz, 2H), 2.68 (t, J = 7.6 Hz, 2H), 2.77−2.83 (m, 1H), 2.83−2.88(m, 1H), 4.20 (s, 1H), 4.35 (s_{br}, 4H), 4.39 (d, J = 5.8, Hz, 2H), 4.47−4.51 (m, 2H), 5.40 (d, J = 4.0 Hz, 1H), 5.52 (dd, J = 8.0, 4.1 Hz, 1H), 5.58 (d, J = 7.9 Hz, 1H), 6.68 (d, J = 8.6 Hz, 2H), 7.16 (d, J = 8.6 Hz, 2H), 7.22 (s, 2H), 7.24 (t, J = 7.9 Hz, 1H), 7.31 (t, J = 7.9 Hz, 2H), 7.35 (dd, J = 8.1, 1.5 Hz, 1H), 7.38 (dd, J = 8.1, 1.5 Hz, 2H), 7.45 (dd, J = 7.8, 1.4 Hz, 1H), 7.53 (dd, J = 7.7, 1.5 Hz, 2H), 7.78 (s, 1H), 8.59 (d, J = 7.9 Hz, 1H), 8.79 (t, J = 6.0 Hz, 2H), 8.95 (t, J = 6.0 Hz, 1H), 9.02 (d, J = 8.0 Hz, 1H), 9.38 (s, 1H), 9.51 (s, 1H), 13.30 (s_{br}, 1H).

^{13}C NMR (176 MHz, DMSO-d_6): δ [ppm] = 20.1, 20.2, 20.3, 24.7, 25.1, 26.6, 30.2, 34.9, 35.2, 39.1, 42.2, 45.6, 55.0, 58.0, 63.7, 67.2, 70.3, 114.9, 121.9, 124.6, 125.4, 125.5, 126.0, 126.0, 126.1, 126.2, 128.1. 128.3, 130.6, 130.6, 131.8, 135.8, 137.5, 140.1, 140.1, 142.8, 146.2, 156.8, 164.5, 164.7, 167.8, 167.9, 168.3, 168.7, 168.9, 170.4, 171.5, 173.5.

$C_{67}H_{68}N_{10}O_{22}S$ (1397.39), exact mass: 1396.4230.

ESI-HRMS (m/z): [M + H]$^+$ calcd for $C_{67}H_{69}N_{10}O_{22}S$: 1397.4309; found: 1397.4285.

Compound ***30***. A mixture of copper(II) sulfate (800 μg, 5.00 μmol, 0.25 equiv) and sodium ascorbate (1.98 mg, 10.0 μmol, 0.5 equiv) in water (100 μL) was added to a solution of **23** (20.5 mg, 30.0 μmol, 1.5 equiv) and **26** (9.25 mg, 20.0 μmol, 1 equiv) in dimethylformamide (500 μL). The solution was stirred for 30 min at rt. The addition of an equal mixture of copper(II) sulfate and sodium ascorbate in water was repeated three times. After each addition, the solution was stirred for 30 min. Compound **30** was obtained by purification of the solution *via* HPLC as a white solid (8.50 mg, 7.42 μmol, 37%).

^{1}H NMR (700 MHz, DMSO-d_6): δ [ppm] = 1.42 (s, 3H), 1.56 (s, 3H), 1.90−1.96 (m, 2H), 2.47 (t, J = 7.4 Hz, 2H), 2.67 (t, J = 7.6 Hz, 2H), 2.77−2.83 (m, 1H), 2.83−2.88 (m, 1H), 4.19 (s, 1H), 4.41 (d, J = 5.8, Hz, 2H), 4.44 (s_{br}, 4H), 4.47−4.55 (m, 2H), 5.40 (d, J = 4.0 Hz, 1H), 5.52 (dd, J = 8.0, 4.0 Hz, 1H), 5.88 (d, J = 7.9 Hz, 1H), 6.61 (t, J = 7.9 Hz, 1H), 6.68 (t, J = 8.0 Hz, 4H), 6.89 (d, J = 7.3, 1H), 6.93 (d, J = 7.8 Hz, 2H), 7.15(d, J = 8.6 Hz, 2H), 7.21(d, J = 7.6 Hz, 1H), 7.21 (s, 2H), 7.30(d, J = 7.7 Hz, 2H), 7.77 (s, 1H), 8.59(d, J = 7.9 Hz, 1H), 9.01(d, J = 8.0 Hz, 1H), 9.09 (s_{br}, 1H), 9.13−9.18 (m, 4H), 9.33 (t, J = 6.0 Hz, 1H), 9.38 (s, 1H),9.55 (s, 1H), 12.53 (s, 2H), 12.58 (s, 1H), 13.23 (s_{br}, 1H).

^{13}C NMR (176 MHz, DMSO-d_6): δ [ppm] = 24.7, 25.1, 26.6, 30.2, 34.8, 35.2, 39.1, 42.1, 45.6, 55.0, 58.0, 63.7, 67.2, 70.3, 114.9, 115.1, 117.1, 117.3, 117.9, 118.0, 118.8, 118.9 121.9, 124.8, 128.1, 128.3, 132.1, 135.9, 137.4, 146.1, 146.2, 146.2, 149.5, 149.6, 156.8, 168.7, 168.9, 169.7, 169.8, 170.4, 171.5, 173.5.

$C_{55}H_{56}N_{10}O_{16}S$ (1145.17), exact mass: 1144.3596.

ESI-HRMS (m/z): [M + H]$^+$ calcd for $C_{55}H_{57}N_{10}O_{16}S$: 1145.3675; found: 1145.3663

Compound ***31a***. *N*-Methylmorpholine (44.0 μL, 40.5 mg, 400 μmol, 4 equiv) and isobutyl chloroformate (32.0 μL, 34.1 mg, 250 μmol, 2.5 equiv) were added to a solution of 4,7,10,13-tetraoxahexadec-15-ynoic acid (78.1 mg, 300 μmol, 3 equiv) in tetrahydrofuran (3 mL) at 0 °C, whereupon a white precipitate formed immediately. The reaction mixture was stirred for 10 min at 0 °C and for 90 min at rt. Compound **21** (100 μmol, 1 equiv) in

https://doi.org/10.1021/acs.jmedchem.1c01482
J. Med. Chem. 2021, 64, 15440−15460

tetrahydrofuran (1 mL) was added at 0 °C over a time of 5 min with a syringe pump. The reaction mixture was stirred overnight at rt, quenched with ice and saturated sodium hydrogen carbonate solution, and extracted with ethyl acetate (3 × 5 mL). The organic layer was washed with hydrochloric acid (0.1 M) and saturated solutions of sodium hydrogen carbonate and sodium chloride (2 × 25 mL each) and dried over sodium sulfate. After removing the solvent, **31a** was obtained by purification *via* HPLC as a white solid (14.5 mg, 13.4 μmol, 13% over 2 steps).

^{1}H NMR (700 MHz, DMSO-d_6): δ [ppm] = 2.16 (s, 3H), 2.17 (s, 6H), 2.28 (s, 3H), 2.28 (s, 6H), 2.62 (t, *J* = 6.2 Hz, 2H), 3.41 (t, *J* = 2.4 Hz,1 H), 3.46−3.54 (m, 12 H), 3.74 (t, *J* = 6.2 Hz, 2H), 4.12 (d, *J* = 2.4 Hz, 2H), 4.35 (s_{br}, 4H) 4.38 (d, *J* = 5.9 Hz, 2H), 7.20 (s, 2H), 7.23 (t, *J* = 7.9 Hz, 1H), 7.31 (t, *J* = 7.9 Hz, 2H), 7.34 (dd, *J* = 8.1, 1.5 Hz, 1H), 7.38 (dd, *J* = 8.1, 1.5 Hz, 2H), 7.44 (dd, *J* = 7.8, 1.5 Hz, 1H), 7.52 (dd, *J* = 7.7, 1.5 Hz, 2H), 8.74 (t, *J* = 6.0 Hz, 2H), 8.94 (t, *J* = 6.0 Hz, 1H), 9.56 (s, 1H).

^{13}C NMR (176 MHz, DMSO-d_6): δ [ppm] = 20.1, 20.2, 20.3, 36.4, 39.1, 42.2, 57.5, 67.0, 68.5, 69.4, 69.6, 69.6, 69.7, 69.7, 77.1, 80.3, 124.6, 125.4, 125.5, 126.0, 126.0, 126.1, 126.2, 130.6, 130.7, 131.8, 136.0, 137.6, 140.1, 142.8, 142.8, 164.5, 164.6, 167.8, 167.9, 168.3, 170.0.

$C_{54}H_{58}N_4O_{20}$ (1083.07), exact mass: 1082.3644.

ESI-HRMS (*m*/*z*): $[M + Na]^+$ calcd for $C_{54}H_{58}N_4NaO_{20}$: 1105.3542 found: 1105.3532.

Compound ***31***. A mixture of copper(II) sulfate (200 μg, 1.25 μmol, 0.17 equiv) and sodium ascorbate (500 μg, 2.50 μmol, 0.33 equiv) in water (50 μL) was added to a solution of **31a** (10.8 mg, 10.0 μmol, 1.33 equiv) and **25** (3.30 mg, 7.5 μmol, 1 equiv) in dimethylformamide (200 μL). The solution was stirred for 30 min at rt. The addition of an equal mixture of copper(II) sulfate and sodium ascorbate in water was repeated three times. After each addition, the solution was stirred for 30 min. Compound **31** was obtained by purification of the solution *via* HPLC as a white solid (9.0 mg, 5.88 μmol, 78%).

^{1}H NMR (700 MHz, DMSO-d_6): δ [ppm] = 1.41 (s, 3H), 1.54 (s, 3H), 2.16 (s, 3H), 2.16 (s, 6H), 2.28 (s, 3H), 2.28 (s, 6H), 2.61 (t, *J* = 6.1 Hz, 2H), 2.81−2.93 (m, 2H), 3.45−3.54 (m, 12 H), 3.73 (t, *J* = 6.2 Hz, 2H), 4.18 (s, 1H), 4.35 (s_{br}, 4H) 4.38 (d, *J* = 5.8 Hz, 2H), 4.47 (s, 2H), 4.50−4.58 (m, 2H), 5.38 (d, *J* = 4.0 Hz, 1H), 5.50, (dd, *J* = 7.8, 4.0 Hz, 1H), 5.72 (d, *J* = 8.1 Hz, 1H), 7.20 (s, 2H), 7.22 (t, *J* = 7.9 Hz, 1H), 7.26 (t, *J* = 7.2 Hz, 1H), 7.30 (t, *J* = 7.5 Hz, 2H), 7.31 (t, *J* = 7.9 Hz, 2H), 7.33−7.36 (m, 3H), 7.37 (dd, *J* = 8.1, 1.4 Hz, 2H), 7.44 (dd, *J* = 7.7, 1.3 Hz, 1H), 7.52 (dd, *J* = 7.7, 1.4 Hz, 2H), 7.96 (s, 1H), 8.72−8.76 (m, 3H), 8.94 (t, *J* = 6.0 Hz, 1H), 9.16 (d, *J* = 7.8 Hz, 1H), 9.58 (s, 1H), 13.38 (s_{br}, 1H).

^{13}C NMR (176 MHz, DMSO-d_6): δ [ppm] = 20.1, 20.1, 20.3, 26.6, 30.4, 35.1, 36.4, 39.1, 42.2, 45.7, 55.4, 58.1, 63.4, 63.8, 67.0, 67.2, 68.9, 69.6, 69.6, 69.7, 69.8, 70.5, 123.9, 124.6, 125.4, 125.5, 126.6, 126.6, 126.1, 126.2, 127.0, 127.5, 128.2, 130.6, 130.7, 131.8, 136.0, 137.6, 137.9, 140.1, 142.8, 142.8, 143.7, 164.5, 164.6, 167.8, 167.9, 168.3, 168.8, 168.9, 169.9, 170.0, 173.3.

$C_{73}H_{80}N_{10}O_{25}S$ (1529.55), exact mass: 1528.5017.

ESI-HRMS (*m*/*z*): $([M + 2H]^{2+}/2)$ calcd for $C_{73}H_{82}N_{10}O_{25}S$: 765.2587; found: 765.2588.

Compound ***32a***. 6-Azidohexoic acid (24.3 mg, 154 μmol, 5 equiv) and *N*-Hydroxysuccinimide (18.5 mg, 161 μmol, 5.2 equiv) were dried *in vacuo* for 20 min and dissolved in dichloromethane (2 mL). *N*,*N*-Dicyclohexylcarbodiimide (33.1 mg, 161 μmol, 5.2 equiv) was added to this solution at 0 °C. The reaction mixture was stirred for 3 h at rt and filtered over celite. Pyridine (15.0 μL, 14.7 mg, 185 μmol, 6 equiv) and daptomycin (50.0 mg, 30.9 μmol, 1 equiv), both dissolved in dimethyl sulfoxide (4 mL), were added to the filtered solution. The reaction mixture was stirred overnight at rt, frozen in liquid nitrogen, and lyophilized. Compound **32a** was obtained by purification of the residue *via* HPLC as a white solid (23.6 mg, 13.4 μmol, 43%).

^{1}H NMR (700 MHz, methanol-d_4): δ [ppm] = 0.89 (t, *J* = 7.2 Hz, 3H), 0.95 (d, *J* = 6.8 Hz, 3H), 1.18−1.27 (m, 10H), 1.23 (d, *J* = 6.5 Hz, 3H), 1.27−1.32 (m, 3H), 1.35 (d, *J* = 7.1 Hz, 3H), 1.36−1.41 (m, 2H), 1.47−1.52 (m, 2H), 1.55−1.64 (m, 6H), 1.65−1.72 (m, 1H), 1.82−1.89 (m, 1H), 2.09−2.15 (m, 1H), 2.15−2.22 (m, 4H), 2.23−2.27 (m, 1H), 2.29−2.36 (d, *J* = 9.1 Hz, 1H), 2.43 (dd, *J* = 15.6, 4.2 Hz, 1H), 2.49−2.59 (m, 3H), 2.75 (dd, *J* = 17.1, 8.7 Hz, 1H), 2.80 (dd, *J* = 17.0, 7.5 Hz, 1H), 2.90−2.96 (m, 2H), 3.12 (dd, *J* = 14.4, 7.1 Hz, 1H), 3.18−3.25 (m, 3H), 3.28 (t, *J* = 6.9 Hz, 2H), 3.49 (dd, *J* = 17.7, 4.5 Hz, 1H), 3.70 (d, *J* = 14.1 Hz, 1H), 3.74−3.80 (m, 2H), 3.84 (d, *J* = 16.9 Hz, 1H), 3.90−4.00 (m, 2H), 4.17 (d, *J* = 16.8 Hz, 1H), 4.23 (q, *J* = 7.0 Hz, 1H), 4.33 (t, *J* = 7.3 Hz, 1H), 4.48 (*J* = 7.7 Hz, 1H), 4.59 (dt, *J* = 12.2, 5.8 Hz, 2H), 4.62−4.64 (m, 1H), 4.65−4.69 (m, 2H), 4.78−4.81 (m, 1H), 5.06−5.10 (m, 1H), 5.33−5.37 (m, 1H), 6.52−6.56 (m, 1H), 6.70 (dd, *J* = 8.4, 0.8 Hz, 1H), 6.97−7.01 (m, 1H), 7.05−7.09 (m, 1H), 7.14 (s, 1H), 7.21 (ddd, *J* = 8.4, 7.0, 1.4 Hz, 1H), 7.32 (d, *J* = 8.1 Hz, 1H), 7.55 (d, *J* = 7.9 Hz, 1H), 7.65 (d, *J* = 8.2 Hz, 1H).

^{13}C NMR (176 MHz, methanol-d_4): δ [ppm] = 14.6, 15.7, 16.4, 17.3, 23.9, 26.7, 26.8, 26.9, 27.6, 28.3, 29.7, 29.8, 30.5, 30.6, 30.7, 33.2, 34.5, 36.2, 36.2, 36.4, 36.8, 37.0, 37.2, 39.5, 39.9, 42.7, 43.8, 44.3, 48.9, 49.8, 50.7, 51.2, 51.4, 51.9, 52.3, 52.5, 55.5, 56.4, 57.4, 57.7, 63.6, 72.1, 110.8, 112.5, 116.6, 118.0, 118.5, 119.5, 120.0, 122.6, 125.0, 128.9, 132.5, 136.3, 138.1, 152.9, 171.0, 171.6, 171.8, 172.3, 172.4, 172.7, 172.9, 173.4, 173.8, 173.8, 173.9, 174.2, 174.2, 174.4, 174.9, 175.1, 175.8, 176.2, 176.2, 176.6, 200.6.

$C_{78}H_{110}N_{20}O_{27}$ (1759.85), exact mass: 1758.7849.

ESI-HRMS (*m*/*z*): $([M + 2H]^{2+}/2)$ calcd for $C_{78}H_{112}N_{20}O_{27}$: 880.4003; found.: 880.4005.

Compound ***32***. A mixture of copper(II) sulfate (680 μg, 4.25 μmol, 0.5 equiv) and sodium ascorbate (1.69 mg, 8.50 μmol, 1 equiv) in water (50 μL) was added to a solution of **23** (11.6 mg, 17.0 μmol, 2 equiv) and **32a** (15.0 mg, 8.50 μmol, 1 equiv) in water (1 mL) and dimethylformamide (300 μL). The solution was stirred for 30 min at rt. The addition of an equal mixture of copper(II) sulfate and sodium ascorbate in water was repeated three times. After each addition, the solution was stirred for 30 min. Compound **32** was obtained by purification of the solution *via* HPLC as a white solid (16.9 mg, 6.93 μmol, 82%).

^{1}H NMR (700 MHz, methanol-d_4): δ [ppm] = 0.88 (t, *J* = 7.2 Hz, 3H), 0.94 (d, *J* = 6.8 Hz, 3H), 1.15−1.31 (m, 18 H), 1.33 (d, *J* = 7.1 Hz, 3H), 1.45−1.51 (m, 2H), 1.51−1.55 (m, 1H), 1.55−1.61 (m, 3H), 1.63−1.69 (m, 1H), 1.79−1.87 (m, 3H), 1.99−2.05 (m, 2H), 2.09 −2.19 (m, 5H), 2.22−2.26 (m, 1H), 2.35 (s_{br}, 1H), 2.43 (dd, *J* = 15.7, 4.3 Hz, 1H), 2.49−2.60 (m, 5H), 2.71−2.82 (m, 4H), 2.89 (dd, *J* = 17.1, 4.7 Hz, 1H), 2.94 (dd, *J* = 17.0, 5.9 Hz, 1H), 3.12 (dd, *J* = 14.3, 7.2 Hz, 1H), 3.16 (t, *J* = 7.0 Hz, 2H), 3.22 (dd, *J* = 114.2, 7.9 Hz, 1H), 3.47 (dd, *J* = 17.6, 4.3 Hz, 1H), 3.68 (d, *J* = 14.7 Hz, 1H), 3.74−3.79 (m, 2H), 3.87 (t, *J* = 15.1 Hz, 2H), 3.94 (d, *J* = 16.9 Hz, 1H), 4.13 (d, *J* = 18.2 Hz, 1H), 4.22 (q, *J* = 7.0 Hz, 1H), 4.28−4.34 (m, 3H), 4.47 (t, *J* = 7.6 Hz, 1H), 4.51−4.58 (m, 7H), 4.60 (t, *J* = 5.6 Hz, 1H), 4.62−4.67 (m, 3H), 4.77−4.80 (m, 1H), 5.04−5.09 (m, 1H), 5.32−5.37 (m, 1H), 6.53 (t, *J* = 7.6 Hz, 1H), 6.55 (t, *J* = 8.8 Hz, 1H), 6.68 (t, *J* = 7.9 Hz, 3H), 6.90 (dd, *J* = 7.8, 1.4 Hz, 1H), 6.92 (dd, *J* = 7.8, 1.3 Hz, 2H), 6.98 (t, *J* = 7.2 Hz, 1H), 7.06 (t, *J* = 7.6 Hz, 1H), 7.13 (s, 1H), 7.15 (dd, *J* = 8.1, 1.2 Hz, 1H), 7.18 (dd, *J* = 8.1, 1.1 Hz, 2H), 7.19−7.22 (m, 1H), 7.31 (d, *J* = 7.6 Hz, 1H), 7.38 (s, 2H), 7.54 (d, *J* = 7.9 Hz, 1H), 7.64 (d, *J* = 8.4 Hz, 1H), 7.65 (s, 1H).

^{13}C NMR (176 MHz, methanol-d_4): δ [ppm] = 14.6, 15.7, 16.5, 17.4, 23.9, 26.0, 26.4, 26.6, 26.8, 26.9, 27.1, 28.3, 29.7, 30.5, 30.6, 30.7, 31.1, 33.2, 34.5, 36.4, 36.5, 36.8, 37.0, 39.5, 39.9, 41.1, 42.6, 43.6, 43.8, 44.3, 48.9, 49.9, 50.8, 51.1, 51.3, 51.4, 51.9, 52.4, 55.5, 56.6, 57.4, 57.8, 63.5, 72.2, 110.8, 112.5, 116.6, 116.7, 116.7, 118.1, 118.5, 118.8, 118.9, 119.5, 119.8, 119.9, 120.0, 122.6, 123.6, 125.0, 128.4, 128.9, 132.5, 133.9, 136.2, 137.6, 138.1, 140.1, 147.4, 147.5, 148.5, 150.5, 152.8, 171.0, 171.6, 171.7, 171.8, 171.9, 172.3, 172.5, 172.7, 173.0, 173.4, 173.8, 174.0, 174.3, 174.4, 174.9, 175.1, 175.7, 175.8, 176.1, 176.3, 176.6, 200.6.

$C_{114}H_{144}N_{24}O_{37}$ (2442.54), exact mass: 2441.0124.

ESI-HRMS (*m*/*z*): $([M + 2H]^{2+}/2)$ calcd for $C_{114}H_{146}N_{24}O_{37}$: 1222.0157; found.: 1222.0159.

https://doi.org/10.1021/acs.jmedchem.1c01482
J. Med. Chem. 2021, 64, 15440−15460

■ ASSOCIATED CONTENT

Supporting Information

The Supporting Information is available free of charge at https://pubs.acs.org/doi/10.1021/acs.jmedchem.1c01482.

Chemical synthesis, biological experiments, analytical data, DFT calculation data; structures and differences in the sum of electronic and zero-point energies between high-spin and low-spin states of natural siderophore−ferric iron complexes; and calculated distances and force constants of Fe−O contacts (O1−O6) in ferric iron complexes of compounds (cpd) **10**, **19**, and **20** (PDF)

■ AUTHOR INFORMATION

Corresponding Author

Mark Brönstrup − *Department of Chemical Biology, Helmholtz Centre for Infection Research, 38124 Braunschweig, Germany; German Center for Infection Research (DZIF), Site Hannover-Braunschweig, 38124 Braunschweig, Germany; Center of Biomolecular Drug Research (BMWZ), Leibniz Universität, 30159 Hannover, Germany;* orcid.org/0000-0002-8971-7045; Email: Mark.Broenstrup@helmholtz-hzi.de

Authors

Lukas Pinkert − *Department of Chemical Biology, Helmholtz Centre for Infection Research, 38124 Braunschweig, Germany*

Yi-Hui Lai − *Department of Chemical Biology, Helmholtz Centre for Infection Research, 38124 Braunschweig, Germany*

Carsten Peukert − *Department of Chemical Biology, Helmholtz Centre for Infection Research, 38124 Braunschweig, Germany*

Sven-Kevin Hotop − *Department of Chemical Biology, Helmholtz Centre for Infection Research, 38124 Braunschweig, Germany*

Bianka Karge − *Department of Chemical Biology, Helmholtz Centre for Infection Research, 38124 Braunschweig, Germany*

Lara Marie Schulze − *Institute for Organic Chemistry, Technical University of Braunschweig, 38106 Braunschweig, Germany*

Jörg Grunenberg − *Institute for Organic Chemistry, Technical University of Braunschweig, 38106 Braunschweig, Germany*

Complete contact information is available at: https://pubs.acs.org/10.1021/acs.jmedchem.1c01482

Author Contributions

L.P. and Y.-H.L. contributed equally to this publication. L.P. performed the chemical experiments and wrote the manuscript. Y.-H.L. conducted biological assays and wrote the manuscript. C.P., S.-K.H., and B.K. conducted biological assays. L.M.S. and J.G. conducted DFT calculations. M.B. conceptualized the study, coordinated the research, and wrote the manuscript. All authors analyzed the results, participated in the final revision of the manuscript, and gave final approval for publication.

Funding

This project was funded by the DFG (grant number: BR 3572/4-1) and the Joint Program Initiative on Antimicrobial Resistance (JPI AMR, grant number: 01KI1825). C.P. thanks the "Fonds der chemischen Industrie" for a scholarship.

Notes

The authors declare no competing financial interest.

■ ACKNOWLEDGMENTS

The authors thank Christel Kakoschke and Ulrike Beutling for their support with NMR and HRMS analytics and Tanja Schickschneit for microbiological experiments.

■ ABBREVIATIONS USED

Amp, ampicillin; Amox, amoxicillin; Cef, cefiderocol; Dapto, daptomycin; Ent, enterobactin; MIC, minimal inhibitory concentration

■ REFERENCES

(1) Tacconelli, E.; Carrara, E.; Savoldi, A.; Harbarth, S.; Mendelson, M.; Monnet, D. L.; Pulcini, C.; Kahlmeter, G.; Kluytmans, J.; Carmeli, Y.; Ouellette, M.; Outterson, K.; Patel, J.; Cavaleri, M.; Cox, E. M.; Houchens, C. R.; Grayson, M. L.; Hansen, P.; Singh, N.; Theuretzbacher, U.; Magrini, N.; Aboderin, A. O.; Al-Abri, S. S.; Awang Jalil, N.; Benzonana, N.; Bhattacharya, S.; Brink, A. J.; Burkert, F. R.; Cars, O.; Cornaglia, G.; Dyar, O. J.; Friedrich, A. W.; Gales, A. C.; Gandra, S.; Giske, C. G.; Goff, D. A.; Goossens, H.; Gottlieb, T.; Guzman Blanco, M.; Hryniewicz, W.; Kattula, D.; Jinks, T.; Kanj, S. S.; Kerr, L.; Kieny, M.-P.; Kim, Y. S.; Kozlov, R. S.; Labarca, J.; Laxminarayan, R.; Leder, K.; Leibovici, L.; Levy-Hara, G.; Littman, J.; Malhotra-Kumar, S.; Manchanda, V.; Moja, L.; Ndoye, B.; Pan, A.; Paterson, D. L.; Paul, M.; Qiu, H.; Ramon-Pardo, P.; Rodríguez-Baño, J.; Sanguinetti, M.; Sengupta, S.; Sharland, M.; Si-Mehand, M.; Silver, L. L.; Song, W.; Steinbakk, M.; Thomsen, J.; Thwaites, G. E.; van der Meer, J. W. M.; Van Kinh, N.; Vega, S.; Villegas, M. V.; Wechsler-Fördös, A.; Wertheim, H. F. L.; Wesangula, E.; Woodford, N.; Yilmaz, F. O.; Zorzet, A. Discovery, research, and development of new antibiotics: the WHO priority list of antibiotic-resistant bacteria and tuberculosis. *Lancet. Infect. Dis.* **2018**, *18*, 318−327.

(2) Theuretzbacher, U.; Gottwalt, S.; Beyer, P.; Butler, M.; Czaplewski, L.; Lienhardt, C.; Moja, L.; Paul, M.; Paulin, S.; Rex, J. H.; Silver, L. L.; Spigelman, M.; Thwaites, G. E.; Paccaud, J. P.; Harbarth, S. Analysis of the clinical antibacterial and antituberculosis pipeline. *Lancet Infect. Dis.* **2019**, *19*, e40−e50.

(3) Zgurskaya, H. I.; Rybenkov, V. V. Permeability barriers of Gram-negative pathogens. *Ann. N. Y. Acad. Sci.* **2020**, *1459*, 5−18.

(4) Masi, M.; Refregiers, M.; Pos, K. M.; Pages, J. M. Mechanisms of envelope permeability and antibiotic influx and efflux in Gram-negative bacteria. *Nat. Microbiol.* **2017**, *2*, No. 17001.

(5) Bassetti, M.; Ginocchio, F.; Mikulska, M. New treatment options against gram-negative organisms. *Crit. Care* **2011**, *15*, 215.

(6) Hider, R. C.; Kong, X. Chemistry and biology of siderophores. *Nat. Prod. Rep.* **2010**, *27*, 637−657.

(7) Krewulak, K. D.; Vogel, H. J. Structural biology of bacterial iron uptake. *Biochim. Biophys. Acta, Biomembr.* **2008**, *1778*, 1781−1804.

(8) Miethke, M.; Marahiel, M. A. Siderophore-based iron acquisition and pathogen control. *Microbiol. Mol. Biol. Rev.* **2007**, *71*, 413−451.

(9) Górska, A.; Sloderbach, A.; Marszall, M. P. Siderophore-drug complexes: potential medicinal applications of the 'Trojan horse' strategy. *Trends Pharmacol. Sci.* **2014**, *35*, 442−449.

(10) Negash, K. H.; Norris, J. K. S.; Hodgkinson, J. T. Siderophore-antibiotic conjugate design: New drugs for bad bugs? *Molecules* **2019**, *24*, No. 3314.

(11) Klahn, P.; Bronstrup, M. Bifunctional antimicrobial conjugates and hybrid antimicrobials. *Nat. Prod. Rep.* **2017**, *34*, 832−885.

(12) Wu, J. Y.; Srinivas, P.; Pogue, J. M. Cefiderocol: A Novel Agent for the Management of Multidrug-Resistant Gram-Negative Organisms. *Infect. Dis. Ther.* **2020**, *9*, 17−40.

(13) Portsmouth, S.; van Veenhuyzen, D.; Echols, R.; Machida, M.; Ferreira, J. C. A.; Ariyasu, M.; Tenke, P.; Nagata, T. D. Cefiderocol versus imipenem-cilastatin for the treatment of complicated urinary tract infections caused by Gram-negative uropathogens: a phase 2, randomised, double-blind, non-inferiority trial. *Lancet Infect. Dis.* **2018**, *18*, 1319−1328.

(14) Pollack, J. R.; Neilands, J. Enterobactin, an iron transport compound from Salmonella typhimurium. *Biochem. Biophys. Res. Commun.* **1970**, *38*, 989−992.
(15) Raymond, K. N.; Dertz, E. A.; Kim, S. S. Enterobactin: an archetype for microbial iron transport. *Proc. Natl. Acad. Sci. U.S.A.* **2003**, *100*, 3584−3588.
(16) Perraud, Q.; Moynie, L.; Gasser, V.; Munier, M.; Godet, J.; Hoegy, F.; Mely, Y.; Mislin, G. L. A.; Naismith, J. H.; Schalk, I. J. A key role for the periplasmic PfeE esterase in iron acquisition via the siderophore enterobactin in *Pseudomonas aeruginosa*. *ACS Chem. Biol.* **2018**, *13*, 2603−2614.
(17) Zheng, T.; Nolan, E. M. Evaluation of (acyloxy)alkyl ester linkers for antibiotic release from siderophore-antibiotic conjugates. *Bioorg. Med. Chem. Lett.* **2015**, *25*, 4987−4991.
(18) Raines, D. J.; Moroz, O. V.; Blagova, E. V.; Turkenburg, J. P.; Wilson, K. S.; Duhme-Klair, A. K. Bacteria in an intense competition for iron: Key component of the Campylobacter jejuni iron uptake system scavenges enterobactin hydrolysis product. *Proc. Natl. Acad. Sci. U.S.A* **2016**, *113*, 5850−5855.
(19) Neumann, W.; Sassone-Corsi, M.; Raffatellu, M.; Nolan, E. M. Esterase-catalyzed siderophore hydrolysis activates an enterobactin-ciprofloxacin conjugate and confers targeted antibacterial activity. *J. Am. Chem. Soc.* **2018**, *140*, 5193−5201.
(20) Zheng, T.; Nolan, E. M. Enterobactin-mediated delivery of beta-lactam antibiotics enhances antibacterial activity against pathogenic *Escherichia coli*. *J. Am. Chem. Soc.* **2014**, *136*, 9677−9691.
(21) Paulen, A.; Hoegy, F.; Roche, B.; Schalk, I. J.; Mislin, G. L. A. Synthesis of conjugates between oxazolidinone antibiotics and a pyochelin analogue. *Bioorg. Med. Chem. Lett.* **2017**, *27*, 4867−4870.
(22) Ghosh, M.; Miller, P. A.; Mollmann, U.; Claypool, W. D.; Schroeder, V. A.; Wolter, W. R.; Suckow, M.; Yu, H.; Li, S.; Huang, W.; Zajicek, J.; Miller, M. J. Targeted Antibiotic Delivery: Selective Siderophore Conjugation with Daptomycin Confers Potent Activity against Multidrug Resistant *Acinetobacter baumannii* Both in Vitro and in Vivo. *J. Med. Chem.* **2017**, *60*, 4577−4583.
(23) Liu, R.; Miller, P. A.; Vakulenko, S. B.; Stewart, N. K.; Boggess, W. C.; Miller, M. J. A synthetic dual drug sideromycin induces gram-negative bacteria to commit suicide with a Gram-positive antibiotic. *J. Med. Chem.* **2018**, *61*, 3845−3854.
(24) Ji, C.; Miller, M. J. Chemical syntheses and in vitro antibacterial activity of two desferrioxamine B-ciprofloxacin conjugates with potential esterase and phosphatase triggered drug release linkers. *Bioorg. Med. Chem.* **2012**, *20*, 3828−3836.
(25) Ferreira, K.; Hu, H. Y.; Fetz, V.; Prochnow, H.; Rais, B.; Muller, P. P.; Bronstrup, M. Multivalent Siderophore-DOTAM Conjugates as Theranostics for Imaging and Treatment of Bacterial Infections. *Angew. Chem., Int. Ed.* **2017**, *56*, 8272−8276.
(26) Oki, N.; Aoki, B.; Kuroki, T.; Matsumoto, M.; Kojima, K.; Nehashi, T. Semisynthetic beta-lactam antibiotics. III. Effect on antibacterial activity and comt-susceptibility of chlorine-introduction into the catechol nucleus of 6-[(R)-2-[3-(3,4-dihydroxybenzoyl)-3-(3-hydroxypropyl)-1-ureido]-2- phenylacetamido]penicillanic acid. *J. Antibiot.* **1987**, *40*, 22−28.
(27) Harris, W. R.; Weitl, F. L.; Raymond, K. N. Synthesis and evaluation of an enterobactin model compound. 1,3,5-Tris-(2,3-dihydroxybenzoylaminomethyl)benzene and its iron(III) complex. *J. Chem. Soc., Chem. Commun.* **1979**, *4*, 177−178.
(28) Venuti, M. C.; Rastetter, W. H.; Neilands, J. B. 1,3,5-Tris(N,N′,N″-2,3-dihydroxybenzoyl)amino-methylbenzene, a synthetic iron chelator related to enterobactin. *J. Med. Chem.* **1979**, *22*, 123−124.
(29) Heidinger, S.; Braun, V.; Pecoraro, V. L.; Raymond, K. N. Iron supply to *Escherichia coli* by synthetic analogs of enterochelin. *J. Bacteriol.* **1983**, *153*, 109−115.
(30) Matzanke, B. F.; Ecker, D. J.; Yang, T. S.; Huynh, B. H.; Muller, G.; Raymond, K. N. *Escherichia coli* iron enterobactin uptake monitored by Mossbauer spectroscopy. *J. Bacteriol.* **1986**, *167*, 674−680.
(31) Kong, H.; Cheng, W.; Wei, H.; Yuan, Y.; Yang, Z.; Zhang, X. An overview of recent progress in siderophore-antibiotic conjugates. *Eur. J. Med. Chem.* **2019**, *182*, No. 111615.
(32) Tao, J.; Perdew, J. P.; Staroverov, V. N.; Scuseria, G. E. Climbing the density functional ladder: nonempirical meta-generalized gradient approximation designed for molecules and solids. *Phys. Rev. Lett.* **2003**, *91*, No. 146401.
(33) Grunenberg, J. The interstitial carbon of the nitrogenase FeMo cofactor is far better stabilized than previously assumed. *Angew. Chem., Int. Ed.* **2017**, *56*, 7288−7291.
(34) Markopoulos, G.; Grunenberg, J. Predicting kinetically unstable C-C bonds from the ground-state properties of a molecule. *Angew. Chem., Int. Ed.* **2013**, *52*, 10648−10651.
(35) Abergel, R. J.; Warner, J. A.; Shuh, D. K.; Raymond, K. N. Enterobactin protonation and iron release: structural characterization of the salicylate coordination shift in ferric enterobactin. *J. Am. Chem. Soc.* **2006**, *128*, 8920−8931.
(36) Zscherp, R.; Coetzee, J.; Vornweg, J.; Grunenberg, J.; Herrmann, J.; Müller, R.; Klahn, P. Biomimetic enterobactin analogue mediates iron-uptake and cargo transport into E. coli and P. aeruginosa. *Chem. Sci.* **2021**, *12*, 10179−10190.
(37) Prochnow, H.; Fetz, V.; Hotop, S. K.; García-Rivera, M. A.; Heumann, A.; Brönstrup, M. Subcellular quantification of uptake in Gram-negative bacteria. *Anal. Chem.* **2019**, *91*, 1863−1872.
(38) Ghosh, M.; Lin, Y.-M.; Miller, P. A.; Möllmann, U.; Boggess, W. C.; Miller, M. J. Siderophore Conjugates of Daptomycin are Potent Inhibitors of Carbapenem Resistant Strains of *Acinetobacter baumannii*. *ACS Infect. Dis.* **2018**, *4*, 1529−1535.
(39) El-Mady, A.; Mortensen, J. E. The bactericidal activity of ampicillin, daptomycin, and vancomycin against ampicillin-resistant *Enterococcus faecium*. *Diagn. Microbiol. Infect. Dis.* **1991**, *14*, 141−145.
(40) Sato, T.; Yamawaki, K. Cefiderocol: Discovery, chemistry, and in vivo profiles of a novel siderophore ephalosporin. *Clin Infect Dis* **2019**, *69*, S538−S543.
(41) Puustinen, A.; Finel, M.; Haltia, T.; Gennis, R. B.; Wikstrom, M. Properties of the two terminal oxidases of *Escherichia coli*. *Biochemistry* **1991**, *30*, 3936−3942.
(42) Thomas, J. W.; Puustinen, A.; Alben, J. O.; Gennis, R. B.; Wikstrom, M. Substitution of asparagine for aspartate-135 in subunit I of the cytochrome bo ubiquinol oxidase of *Escherichia coli* eliminates proton-pumping activity. *Biochemistry* **1993**, *32*, 10923−10928.
(43) Abramson, J.; Riistama, S.; Larsson, G.; Jasaitis, A.; Svensson-Ek, M.; Laakkonen, L.; Puustinen, A.; Iwata, S.; Wikström, M. The structure of the ubiquinol oxidase from *Escherichia coli* and its ubiquinone binding site. *Nat. Struct. Biol.* **2000**, *7*, 910−917.
(44) Braun, V. Surface signaling: novel transcription initiation mechanism starting from the cell surface. *Arch. Microbiol.* **1997**, *167*, 325−331.
(45) Faraldo-Gómez, J. D.; Sansom, M. S. Acquisition of siderophores in gram-negative bacteria. *Nat. Rev. Mol. Cell Biol.* **2003**, *4*, 105−116.
(46) Baker, K. R.; Postle, K. Mutations in *Escherichia coli* ExbB transmembrane domains identify scaffolding and signal transduction functions and exclude participation in a proton pathway. *J. Bacteriol.* **2013**, *195*, 2898−2911.
(47) Skare, J. T.; Ahmer, B. M.; Seachord, C. L.; Darveau, R. P.; Postle, K. Energy transduction between membranes. TonB, a cytoplasmic membrane protein, can be chemically cross-linked in vivo to the outer membrane receptor FepA. *J. Biol. Chem.* **1993**, *268*, 16302−16308.
(48) Shaik, S.; Kumar, D.; de Visser, S. P.; Altun, A.; Thiel, W. Theoretical perspective on the structure and mechanism of cytochrome P450 enzymes. *Chem. Rev.* **2005**, *105*, 2279−2328.
(49) Kim, A.; Kutschke, A.; Ehmann, D. E.; Patey, S. A.; Crandon, J. L.; Gorseth, E.; Miller, A. A.; McLaughlin, R. E.; Blinn, C. M.; Chen, A.; Nayar, A. S.; Dangel, B.; Tsai, A. S.; Rooney, M. T.; Murphy-Benenato, K. E.; Eakin, A. E.; Nicolau, D. P. Pharmacodynamic Profiling of a Siderophore-Conjugated Monocarbam in *Pseudomonas*

https://doi.org/10.1021/acs.jmedchem.1c01482
J. Med. Chem. 2021, 64, 15440−15460

aeruginosa: Assessing the Risk for Resistance and Attenuated Efficacy. *Antimicrob. Agents Chemother.* **2015**, *59*, 7743−7752.
(50) Tomaras, A. P.; Crandon, J. L.; McPherson, C. J.; Banevicius, M. A.; Finegan, S. M.; Irvine, R. L.; Brown, M. F.; O'Donnell, J. P.; Nicolau, D. P. Adaptation-based resistance to siderophore-conjugated antibacterial agents by *Pseudomonas aeruginosa*. *Antimicrob. Agents Chemother.* **2013**, *57*, 4197−4207.
(51) Kopp, D. R.; Postle, K. The intrinsically disordered region of ExbD is required for signal transduction. *J. Bacteriol.* **2020**, *202*, No. e00687-19.
(52) Wikström, M.; Bogachev, A.; Finel, M.; Morgan, J. E.; Puustinen, A.; Raitio, M.; Verkhovskaya, M.; Verkhovsky, M. I. Mechanism of proton translocation by the respiratory oxidases. The histidine cycle. *Biochim. Biophys. Acta, Bioenerg.* **1994**, *1187*, 106−111.
(53) Price, C. E.; Driessen, A. J. M. Biogenesis of membrane bound respiratory complexes in *Escherichia coli*. *Biochim. Biophys. Acta, Mol. Cell Res.* **2010**, *1803*, 748−766.
(54) Keren, I.; Kaldalu, N.; Spoering, A.; Wang, Y.; Lewis, K. Persister cells and tolerance to antimicrobials. *FEMS Microbiol. Lett* **2004**, *230*, 13−18.
(55) Lázár, V.; Pal Singh, G.; Spohn, R.; Nagy, I.; Horváth, B.; Hrtyan, M.; Busa-Fekete, R.; Bogos, B.; Méhi, O.; Csörgő, B.; Pósfai, G.; Fekete, G.; Szappanos, B.; Kégl, B.; Papp, B.; Pál, C. Bacterial evolution of antibiotic hypersensitivity. *Mol. Syst. Biol.* **2013**, *9*, No. 700.

https://doi.org/10.1021/acs.jmedchem.1c01482
J. Med. Chem. 2021, 64, 15440−15460